The Journal of Antibiotics (2018) 71, 215–233

www.nature.com/ja

REVIEW ARTICLE

Challenges and discoveries in the total synthesis of complex polyketide natural products

Ian Paterson and Nelson Yuen Sum Lam

Structurally complex polyketide natural products, isolated from a variety of marine and terrestrial sources, continue to provide a valuable source of rewarding targets for the synthetic chemist to tackle. In this account, we provide an overview of the total synthesis of several structurally fascinating polyketides with promising anticancer activity completed in our group based on our versatile asymmetric aldol methodology—spirastrellolide A methyl ester, leiodermatolide, rhizopodin and chivosazole F—and highlight the unanticipated challenges and discoveries encountered.
The Journal of Antibiotics (2018) **71,** 215–233; doi:10.1038/ja.2017.111; published online 25 October 2017

INTRODUCTION

Through aeons of evolution, nature has gifted us with a seemingly limitless source of important secondary metabolites. Such compounds are often astoundingly intricate in terms of their molecular architecture, with stereochemically elaborate scaffolds that dwarf structures conceived by mankind. Unsurprisingly, such extraordinary structures demand effective methodologies and strategies, along with hard work and perseverance, to ensure a successful outcome from a suitably focused synthetic campaign. Furthermore, the vanishingly low isolation yields of such natural products can preclude their full stereochemical assignment, rendering total synthesis a valuable tool for structural elucidation.[1–5]

Among the vast chemical space carved out by nature are the polyketides, typified by their dazzling array of functionality and stereochemistry, providing a testing intellectual challenge for the synthetic chemist. Enticed by these intriguing structures, which generally have impressive biological activities,[6] our group has had a longstanding interest in the development of novel synthetic methods and strategies that are both robust and, where required, flexible. In this context, the efficiency of our suite of versatile boron-mediated aldol reactions has proved invaluable for the controlled installation of the highly oxygenated frameworks of these captivating natural products.[7–9]

In this account, we provide an overview of recent research endeavors that have culminated in the total synthesis of several challenging polyketide natural products with promising anticancer activity in our group: spirastrellolide A methyl ester (**1**), leiodermatolide (**2**), rhizopodin (**3**) and chivosazole F (**4**) (Figure 1). In particular, we highlight the unexpected obstacles encountered and subsequent discoveries that resulted in the successful total syntheses of these highly challenging targets.

SPIRASTRELLOLIDE A METHYL ESTER

The spirastrellolides constitute an extraordinary family of spiroacetal macrolides first isolated by Andersen and co-workers[10] in 2003 from extracts of the Caribbean sponge *Spirastrella coccinea*. The most abundant congener, spirastrellolide A (**1**) (isolated as the corresponding methyl ester), exhibits striking structural complexity, containing 20 stereocenters, a 38-membered macrolactone and a nine-carbon side chain featuring a (*Z*,*E*)-1,4-diene.[11–15] The macrocycle itself contains a tetrahydropyran (A ring), a bicyclic 6,6-spiroacetal (BC rings) and a tricyclic 5,6,6-spiroacetal (DEF rings) featuring a chlorine atom at C28. Additionally, spirastrellolide A was found to exhibit potent antimitotic properties via selective protein phosphatase 2A inhibition ($IC_{50} = 1$ nM).[10,12] Beyond the obvious potential as a novel anticancer lead, such phosphatase inhibitors have also shown therapeutic promise in tackling obesity, autoimmune conditions and neurodegenerative disorders.[16] The combination of the synthetic challenge posed by their architectural complexity and promising biological activity has rendered the spirastrellolides the focus of intense research efforts from numerous groups.[15] Despite this, only five completed syntheses have been reported to date,[17–20] two of which are from our group.[21–24]

Our efforts toward spirastrellolide A methyl ester began soon after disclosure of the originally proposed structure and our synthetic approach evolved concurrently with structural determination studies on this moving target.[25] A flexible endgame was a strict requirement as a consequence of the ambiguity surrounding the C46 hydroxyl stereocenter. Specifically, our initial strategy in face of these imposed requirements involved a modular approach to macrocycle formation, resulting in the successful assembly of the complete ABCDEF ring system, followed by late-stage side-chain attachment to facilitate preparation of both possible C46 diastereomers.[26]

With advanced intermediate **5** (Scheme 1) in hand after a sustained campaign of dedicated efforts,[22,26] synthesis completion appeared

University Chemical Laboratory, Cambridge, UK
Correspondence: Professor I Paterson, University Chemical Laboratory, Lensfield Road, Cambridge CB2 1EW, UK.
E-mail: ip100@cam.ac.uk
Received 9 May 2017; revised 25 July 2017; accepted 4 August 2017; published online 25 October 2017

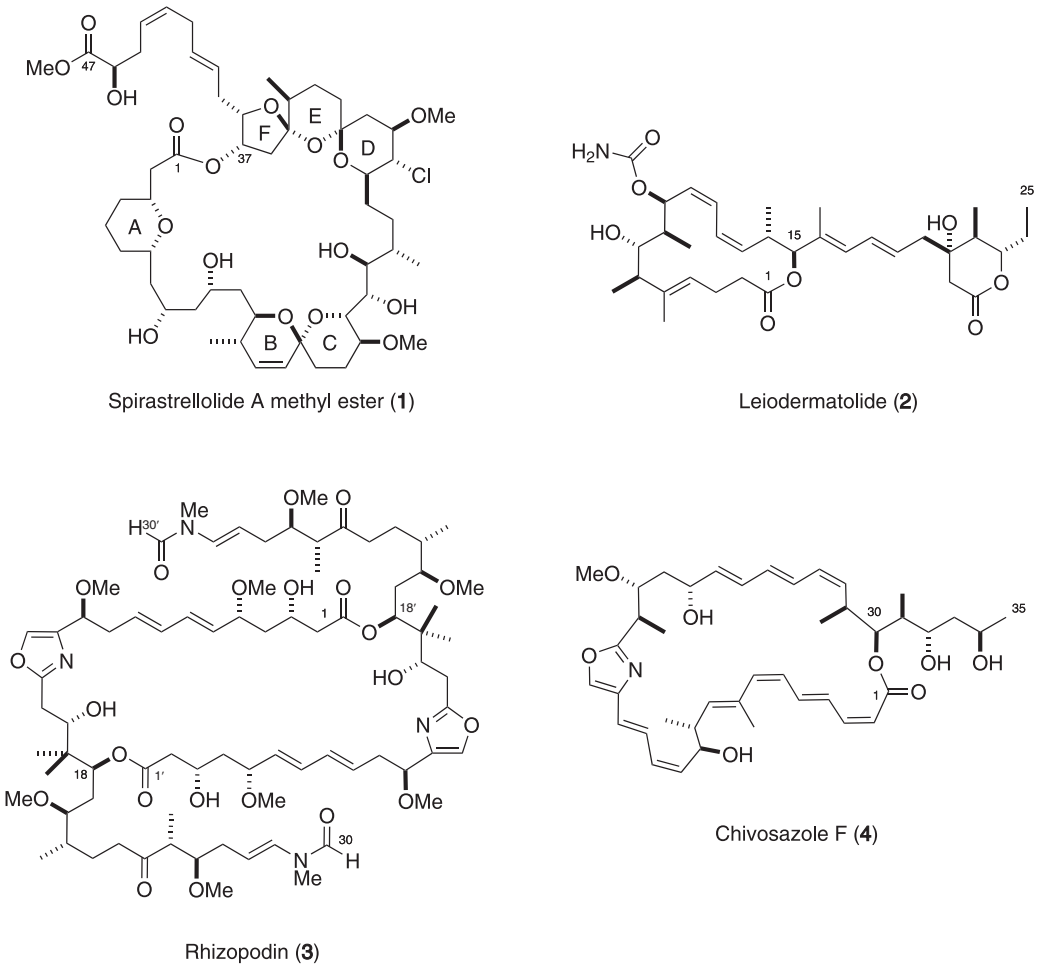

Figure 1 Structures of spirastrellolide A methyl ester (**1**), leiodermatolide (**2**), rhizopodin (**3**) and chivosazole F (**4**).

tantalizingly close. Unfortunately, selective removal of the C40 silyl-protecting group to enable side-chain incorporation proved to be a major obstacle. In the end, a global deprotection, followed by protecting group adjustment, was required. Oxidation to the corresponding aldehyde **6** then proceeded smoothly and set the scene for homologation. At this point, a variety of organometallic addition reactions were trialed unsuccessfully. We surmised that these failures were likely to be a reflection of the steric constraints imposed on the C40 aldehyde by the proximal cage-like macrocycle. After exhaustive experimentation, it was found that a simple Wittig olefination reaction could be used to access a terminal alkene, thereby allowing side-chain incorporation via olefin cross-metathesis.[27,28] After considerable experimentation, the cross-metathesis with dicarbonate **7** required relatively forcing conditions (refluxing in benzene), due to the steric constraints imposed by the macrocycle. The resulting allylic carbonate **8** then allowed a π-allyl Stille cross-coupling with stannane **9** to afford the *bis*-acetonide protected natural product, which underwent a global deprotection to afford the first total synthesis of spirastrellolide A methyl ester (**1**).[22] Notably, the 46-*epi* diastereomer of **1** showed distinctly different NMR spectra due to the influence of the proximate macrocycle.

Having successfully completed the target molecule, and thereby validating the configurational assignment, we next sought to improve our synthesis, paying specific attention to avoiding unnecessary redox steps and protecting group manipulations. In particular, the need for a divergent side-chain installation strategy was now deemed unnecessary with the stereochemistry of the natural product now unambiguously assigned. Additionally, we sought to capitalize on the availability of key fragments from our first-generation approach, giving rise to the revised retrosynthetic analysis in Scheme 2. Notably, we looked to establish the C1-C47 carbon backbone in **10** (from allylic carbonate **11** and stannane **12**) in its entirety before macrolactonization, thereby simplifying incorporation of the (*E*,*Z*)-skipped diene side chain. Building on earlier work, the BC-spiroacetal moiety would be installed through 4-methoxybenzyl (PMB) deprotection/*in situ* spiroacetalization of a *Z*-enone arising from coupling of the C1-C16 alkyne fragment **13** and C17-C40 aldehyde **14**.[26] Disconnection across C24-C25 via an sp^3-sp^2 Suzuki coupling[29] then reveals two intermediates utilized previously, C17-C24 vinyl iodide **15** and C25-C40 *bis*-spiroacetal **16**.[30]

In our first-generation synthesis, the construction of the C26-C40 DEF *bis*-spiroacetal **17** via an acid-mediated deprotection/spiroacetalization cascade of **18** was a major bottleneck.[31] The problem stemmed from formation of the undesired furan **19** via competing elimination (Scheme 3a). Even after extensive optimization, we could only generate a modest amount of the required C26-C40 DEF *bis*-spiroacetal **17**. Thus, we needed to revise our strategy to achieve a reliable multigram supply of this essential fragment. First, we removed the appended γ-lactone in a bid to avoid competitive furan formation. Additionally, we noted that the *bis*-spiroacetal could arise from a

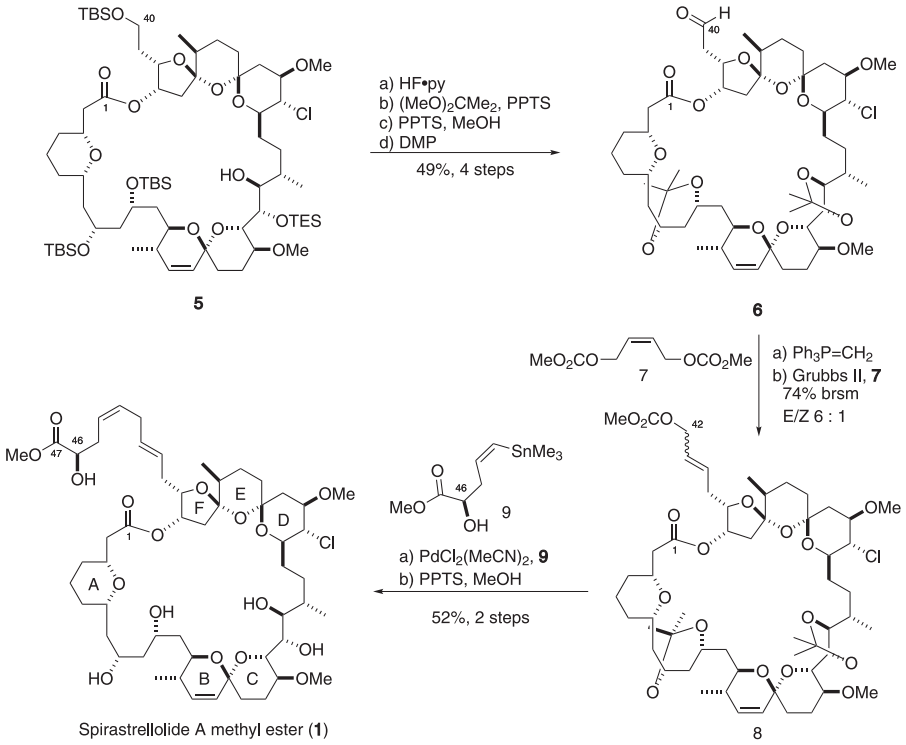

Scheme 1 Endgame sequence for the first-generation synthesis of spirastrellolide A methyl ester (**1**).

tetraol linear precursor. In particular, we recognized that the sense of asymmetric induction via the Sharpless asymmetric dihydroxylation required to install the C37/C38 and C26/C27 hydroxyls was the same. This led to an adventurous double dihydroxylation/spiroacetalization cascade as in **20** to **21**, which, if successful, would provide an elegant and efficient synthesis of the DEF *bis*-spiroacetal ring system (Scheme 3b).

The required linear precursor **20** (Scheme 4) was readily prepared from aldehyde **22** and ketone **23**, notably using an Oehlschlager–Brown *syn*-choroallylation[32] and our lactate aldol methodogy[33] to set up the required stereocenters.[24] A boron-mediated aldol reaction facilitated the fragment union to form β-hydroxyketone **24**, which led onto the required linear precursor **20** via a four-step sequence.[30] At this stage, we attempted the pivotal double asymmetric dihydroxylation.[34] This initially afforded *bis*-hemiacetal **25**, which to our delight spirocyclized under mild acidic conditions to afford the DEF *bis*-spiroacetal **21**. Fortuitously, we discovered that other spirocyclic isomers of **21** could be resubmitted under acidic conditions to afford the required DEF *bis*-spiroacetal cleanly. This was only made possible by the increased stability of the DEF *bis*-spirocycle circumventing furan formation, giving us the opportunity to use thermodynamic equilibration rather than kinetic control. A final *bis*-silylation delivered the protected fragment **26** efficiently. Most importantly, this route facilitated a dependable multigram scale synthesis of the crucial C26-C40 *bis*-spiroacetal moiety.

Armed with an efficient and scalable route towards C1-C16 alkyne **13**, C17-24 vinyl iodide **15** and now the C26-C40 *bis*-spiroacetal **26**,[26,30] we set out to improve the fragment coupling sequence (Scheme 5).[35] Preparation of C17-C40 aldehyde **14** commenced with a primary triethylsilyl (TES) deprotection, oxidation and methylenation to provide the corresponding C25-C40 alkene **16**. Hydroboration of **16** followed by an *in situ* sp^3-sp^2 Suzuki cross-coupling with vinyl iodide **15** forged the C24-C25 bond and furnished diene **27** cleanly.[29,36] The final two stereocenters of the C17-C40 fragment were set up via a diastereoselective substrate-controlled double hydroboration sequence; installing the C17 and C23 hydroxyl groups and affording the required 23,24-*anti* stereochemistry in **28**. Protecting group manipulations then yielded an advanced triol, which was subjected to a selective triple oxidation of the two primary alcohols with concomitant lactonization to afford the required C17-C40 aldehyde **14**.

Our initial coupling strategy to form the C16-C17 bond hinged upon an the addition of an alkynyllithium species to the C17 aldehyde.[26] However, this transformation now proved to be capricious owing to competing addition to the γ-lactone moiety. Instead, a Nozaki–Hiyama–Kishi coupling[37,38] between iodoalkyne **29** and aldehyde **14**, to our delight, chemoselectively and reliably forged the C16-C17 bond (Scheme 6). The BC-spiroacetal formation commenced with a Lindlar reduction of the alkyne **30** and oxidation to the *Z*-enone. Subsequent *bis*-PMB deprotection under controlled conditions set the scene for a concomitant acetalization to cleanly forge the BC-spiroacetal ring system, now affording **31** with all the requisite ABCDEF rings in a stereodefined manner. With the carbon and oxygen skeleton for the macrocycle now in hand, our attention turned towards side-chain installation and the final macrolactonization. A selective primary TBS ether deprotection, partial reduction of the γ-lactone and vinylation afforded allylic alcohol **32**, which was then treated with triphosgene to both temporarily mask the diol as well as providing the requisite leaving group for the π-allyl Stille cross-coupling. Pleasingly, the planned cross-coupling between allylic carbonate **11** and vinyl stannane **12** proceeded efficiently, and was a major improvement over our previous cross-metathesis route in the presence of the full macrocycle. With only the macrolactonization and

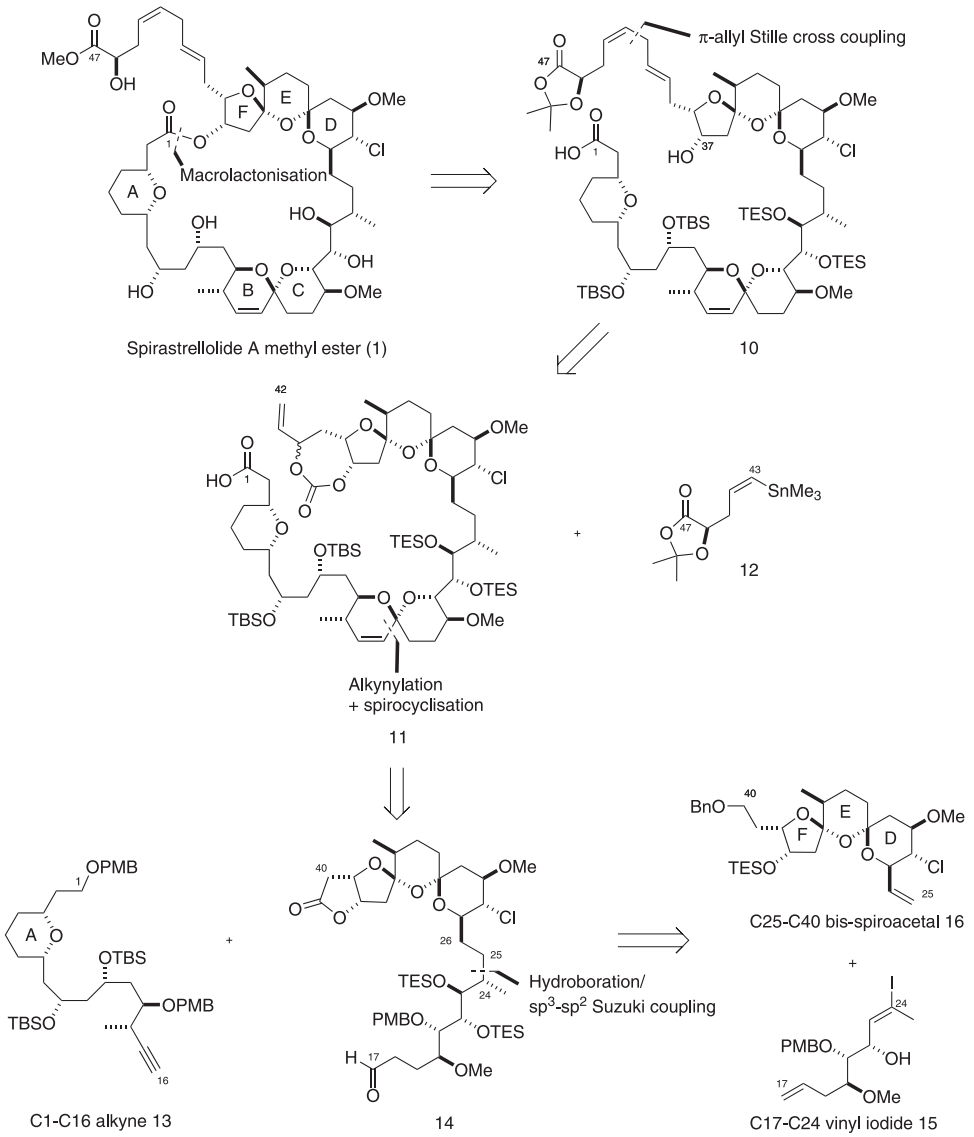

Scheme 2 Revised retrosynthesis of spirastrellolide A methyl ester (**1**).

global deprotection left, the finish line was now in sight. Once again, this transformation proved to be significantly more challenging than initially anticipated!

Frustratingly, subjecting *seco*-acid **10** to increasingly forcing conditions (including refluxing in toluene) for macrolactonization[39,40] not only failed to furnish the cyclized product, but returned degraded starting material. We initially surmised that the side chain was perhaps impeding the macrolactonization; however, diol **33** corresponding to the truncated macrocycle also failed to cyclize when subjected to previously established macrolactonization conditions (Scheme 7a). This unexpected difficulty was in stark contrast to the highly efficient macrolactonization (>95%) observed in our first-generation route (Scheme 7b), which we attributed to a degree of favorable conformational preorganization in the *seco*-acid **34**. Comparison of the *seco*-acid **10** with that used previously highlighted only one seemingly minor structural difference—the (very distal) C23-TES ether. Therefore, we hypothesized that unfavorable conformational effects, presumably imposed by the additional silyl-protecting group, were operating to bias the free acid away from ring closing with the C37 alcohol. As such, we treated *seco*-acid **10** with pyridinium *p*-toluenesulfonate in methanol to effect controlled *mono*- and *bis*-TES ether cleavage. Our hypothesis was proven to be correct; submitting either of the *mono*- or *bis*-desilylated products (**35** and **36**) to standard Yamaguchi macrolactonization conditions now afforded macrocycles **37** and **38** in excellent yield (Scheme 7c). A final global deprotection completed our second-generation synthesis of spirastrellolide A methyl ester (**1**) in 23 linear steps and 6% overall yield from C26-C40 *bis*-spiroacetal **26**. When compared with the first-generation synthesis (25 steps and 1% overall yield), it is pleasing to note the improvement in efficiency, both in terms of step count and yield. Moreover, we discovered that we were incredibly lucky in our first-generation synthesis—where the troublesome C23-TES ether was unintentionally cleaved in the BC-spiroacetalization step, which greatly assisted the crucial downstream macrolactonization reaction. An important lesson was learned here that protecting groups can have subtle and unpredictable conformational effects in such complex substrates!

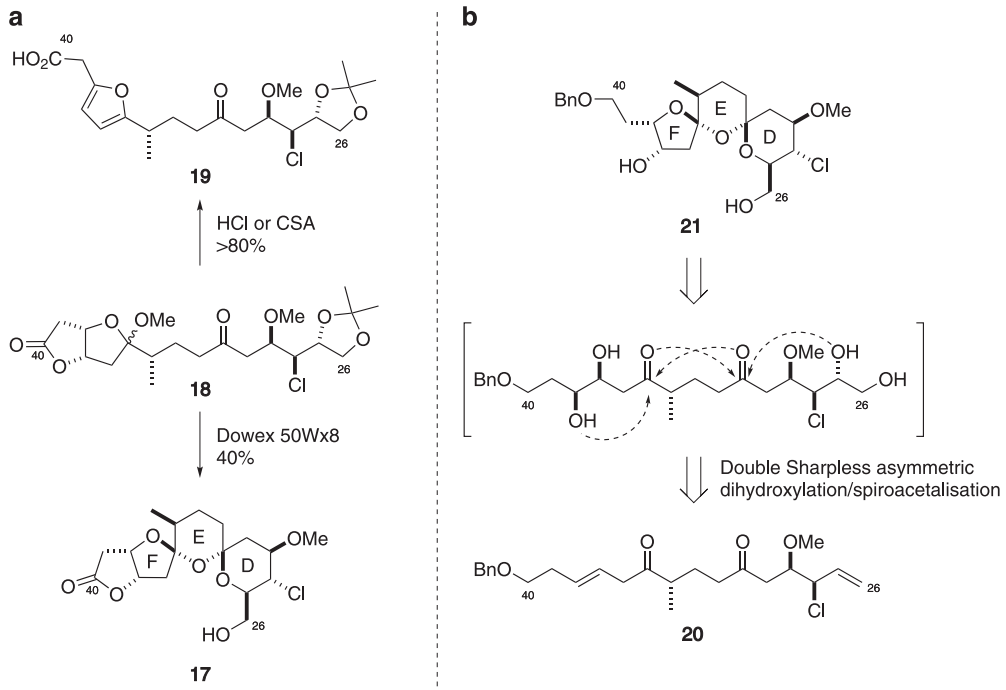

Scheme 3 (**a**) First-generation approach towards the C26-C40 DEF *bis*-spiroacetal **17**. (**b**) Revised strategy towards the C26-C40 DEF *bis*-spiroacetal **21**.

LEIODERMATOLIDE

In 2008, leiodermatolide (**2**) was isolated from the lithistid sponge *Leiodermatium* sp. collected off the coast of Florida by the Wright group.[41] Spectroscopic analysis illuminated the planar structure of **2** and revealed a 16-membered macrolactone containing a *Z,Z*-diene and a pendant carbamate group, as well as an *E,E*-diene on the side chain terminating in a δ-lactone. The assigned structure highlighted the presence of nine stereocenters; six of which lie in the macrocycle and three in the terminal *δ*-lactone.[42] Biological evaluation showed that leiodermatolide exhibited potent anticancer activity, in particular against a range of drug-resistant cancer cell lines. While leiodermatolide-treated cells exhibited physiological responses often typified by tubulin-binding compounds, *in vitro* studies failed to show evidence for any direct tubulin interaction. As such, it was suggested that leiodermatolide acted via an indirect mechanism orthogonal to other known tubulin-targeting anticancer drugs, indicative of a promising anticancer drug candidate.

Our involvement with leiodermatolide was borne from its initially inconclusive stereochemical assignment. In collaboration with the Wright group, extensive NMR spectroscopic analysis, molecular modeling and computational DP4 NMR predictions[43] allowed us to refine the structure to a single diastereomer for the C1-C16 macrocycle and the C21-C25 *δ*-lactone with >99% probability. Unfortunately, the distal nature of the C21-C25 *δ*-lactone relative to the macrocycle precluded a conclusive determination of the stereochemistry between these two stereoclusters, leading to four candidate stereoisomers for the natural product. To definitively pin down the stereochemistry of **2**, we embarked on a synthetic campaign geared towards confirming the three-dimensional structure of the macrocycle followed by the full natural product. A synthesis-enabled stereochemical elucidation was a notion shared with other research groups,[44,45] which, to date, has resulted in one other group successfully synthesizing leiodermatolide.[46,47]

As the absolute configuration was unknown, we arbitrarily targeted *ent*-**2** and its diastereomer for initial studies. Our initial approach towards **2** hinged upon a late-stage sp^2-sp^2 Suzuki coupling across C17-C18 to allow the flexible appendage of both enantiomers of the C18-C25 *δ*-lactone to the macrocycle, as shown in Scheme 8a. The C18-C25 *δ*-lactone **39** could be readily synthesized from either enantiomer of **40**. We anticipated that the C1-C17 macrocycle **41** could be constructed from a linchpin *bis*-halide fragment **42**, leveraging the more reactive vinyl iodide to selectively engage in a Stille cross-coupling with C1-C11 vinyl stannane **43**.

In executing this approach (Scheme 8b), we discovered that the *bis*-TBS protection of the C7 and C9 hydroxyl groups required relatively forcing conditions to effect the second silylation at C7.[48] This observation indicated the possibility of realizing a site-selective C9 carbamate installation in the endgame. Our resulting synthesis of the C1-C17 macrocycle **41** confirmed our relative stereochemical assignment through spectroscopic correlations.[48] However, the specific rotation recorded for the macrocycle was opposite in sign to (−)-leiodermatolide, tentatively suggesting that we may have embarked in the wrong enantiomeric series. Additionally, there were two key issues we needed to address in the evolution of our synthetic strategy. First, while the semireduction of vinyl dibromide **44** to (*Z*)-vinyl bromide **45** proceeded smoothly, subsequent attempts at converting it into the vinyl stannane proved problematic. This involved cleavage of the C7 and C9-TBS ethers to afford diol **46**, followed by stannylation under Wulff–Stille conditions[49] to form stannane **43**, albeit in a modest yield (Scheme 6b). Furthermore, despite preliminary results suggesting otherwise, our vision of a late-stage site-selective carbamate installation proved unrewarding; treatment of the macrocycle **47** with trichloroacetyl isocyanate[50] resulted in a 3:2 mixture of regioisomeric products **41** and **48** that favored the undesired C7 carbamate **48**. Moreover, attempts at realizing the key Suzuki coupling to afford the full leiodermatolide carbon skeleton proved fruitless; vinyl bromide **41**

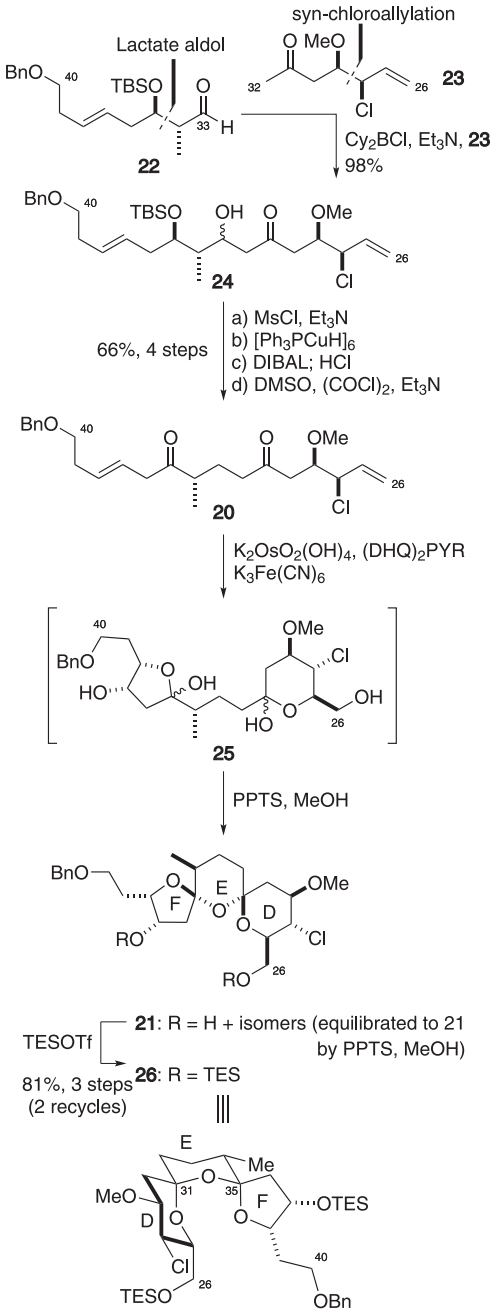

Scheme 4 Revised synthesis of the C26-C40 DEF *bis*-spiroacetal **26**.

was found to be unreactive under a variety of palladium-catalyzed conditions.[51]

This intelligence gathering exercise prompted us to revise our synthetic strategy towards **2**, as highlighted in Scheme 9, and we instead looked towards forming the fully elaborated macrocycle via a late-stage macrolactonization. As the C11-C12 bond was reliably installed via a Stille coupling, we sought to disconnect the molecule into the C1-C11 vinyl stannane *ent*-**43** and the C12-C25 δ-lactone **49**. The C12-C25 fragment itself can then be constructed from vinyl iodide **50** and δ-lactone *ent*-**39**, using a Suzuki coupling to forge the C17-C18 bond. Despite disappointing initial results, we remained optimistic about effecting a regioselective carbamate formation, thereby minimizing protecting group manipulations.

Our revised synthesis of the C1-C11 stannane *ent*-**43** commenced from the Weinreb amide **51** derived from (*R*)-Roche ester (Scheme 10). By trapping the kinetic *Z*-enolate of the derived ketone with Comins' reagent[52] followed by a Suzuki-type methylation of vinyl triflate **52**, we successfully formed the trisubstituted alkene **53**.[53] Using methodology developed by our group, a lactate aldol reaction between (*R*)-lactate-derived ethyl ketone (*R*)-**40** and aldehyde **54** readily afforded the required *anti* adduct **55** with excellent diastereoselectivity.[33,54,55] A four-step sequence installed the requisite alkyne and removed the lactate auxiliary. The required 1,3-*anti* reduction on ynone **56** proved problematic, using the Evans–Tishchenko[56] protocol failed outright. Unfortunately, the Evans–Saksena reduction[57] on the same substrate gave poor diastereoselectivity. This was rationalized based on the small size of the alkyne substituent, reducing its preference to occupy the equatorial position in the transition state. Based on this hypothesis, we looked towards increasing the steric bulk by preparing the *Z*-vinyl iodide **57**.[58] Luckily, this drastically improved the selectivity of the 1,3-*anti* reduction via the Evans–Saksena protocol, completing the required stereotetrad in the C1-C11 fragment. Next, lithiation followed by trapping with tributyltin chloride proceeded smoothly to give the C1-C11 stannane **58**. Gratifyingly, this route was a significant improvement over our initial approach (20% yield over 14 steps, versus 6% yield over 14 steps).[48,59]

The C12-C17 vinyl iodide was constructed again using our lactate aldol methodology, furnishing **50** in four steps (via aldol adduct **59**) from ethyl ketone (*S*)-**40** (Scheme 11).[33,54,55] Synthesis of the C18-C25 *δ*-lactone commenced with a boron-mediated aldol reaction between ketone (*R*)-**40** and propanal, affording the required *anti* adduct **60**. The *δ*-lactone was constructed through a $BF_3{\cdot}OEt_2$-mediated Mukaiyama aldol reaction between ketone **61** and silyl ketene acetal **62**.[8,60] This, followed by an acid-mediated lactonization, delivered the δ-lactone **63**, where the matched stereoinduction from 1,2-Felkin and 1,3-Evans polar models are mutually reinforcing.[61] Subsequent silylation afforded the protected lactone **64**, where a two-step sequence revealed the required vinyl boronate *ent*-**39** in anticipation for the key cross-coupling.

The planned Suzuki coupling could be effected between vinyl iodide **50** and vinyl boronate *ent*-**39**. Advantageously, we discovered that the fragment union could also be readily achieved with excellent geometrical control via the Heck reaction to deliver **65** (Scheme 12),[62] saving two steps in converting the alkene **64** to the vinyl boronate *ent*-**39** (*vide supra*). A two-step procedure revealed the required C12-C25 vinyl iodide **49**, which underwent a facile Stille coupling[63,64] with stannane **58** to establish **66**, corresponding to the full carbon skeleton of leiodermatolide. Finally, a series of redox and protecting group manipulations revealed the *seco*-acid **67**, which was efficiently macrocyclized under our preferred Yamaguchi conditions[39] to generate the 16-membered macrolactone.

With a global deprotection revealing the *des*-carbamoyl derivative of leiodermatolide **68**, all that was required was the pivotal regioselective C9 carbamoylation. We surmised that the steric hindrance around C7 should heighten the reactivity of the C9 alcohol, a rationale supported by molecular modeling studies. As previously alluded to, treating the truncated macrolactone **47** with trichloroacetyl isocyanate[50] favored the formation of the undesired C7 carbamate **48**, with extensive experimentation failing to overturn this result. Interestingly enough, we observed that esterification or silylation proceeded with high selectivity at the C9 position. This hinted that it was indeed the more reactive position, with the carbamoylating agent behaving

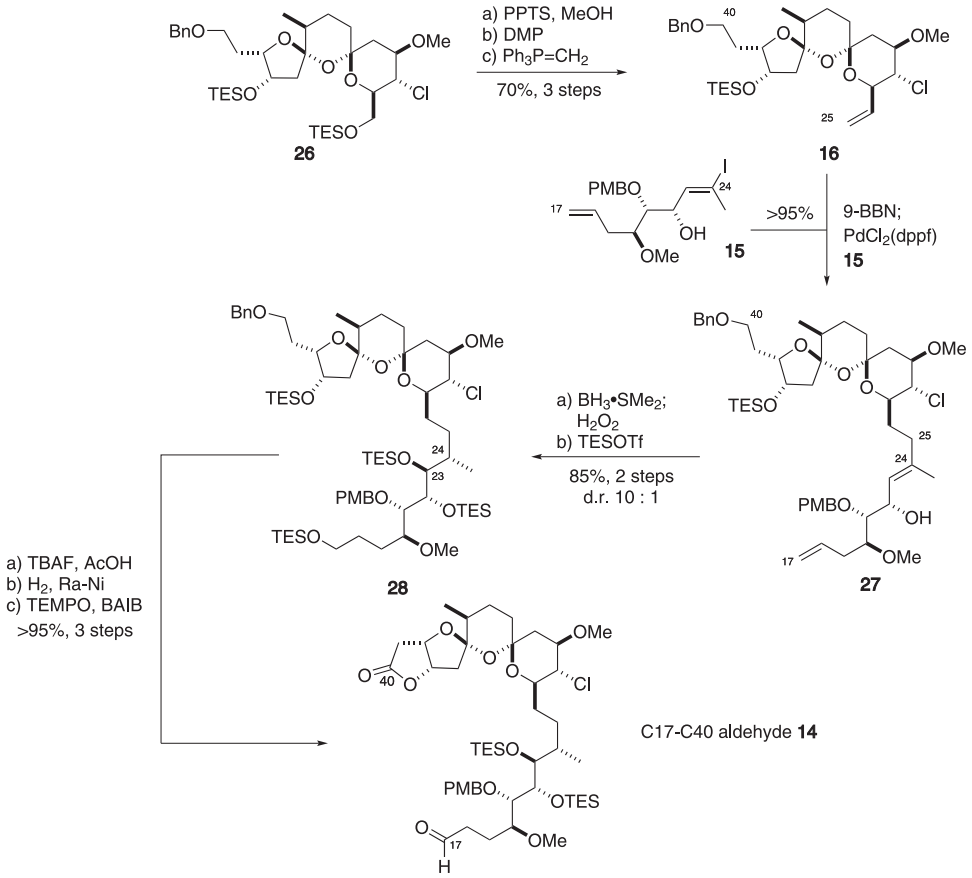

Scheme 5 Synthesis of the C17-C40 aldehyde **14**.

anomalously. Leveraging this finding, a sequence involving *bis*-silylation, selective C9 desilylation, followed by treatment with trichloroacetyl chloride and C7 desilylation successfully led to (−)-leiodermatolide (**2**) in 23 steps and 3.2% overall yield.[59] Careful comparison with the authentic sample provided by the Wright group confirmed that they were identical in all respects. Serendipitously, this three-dimensional structure corresponds exactly to the one out of four stereoisomers arbitrarily rendered in our isolation paper.[42] At this point, we could embark on a program of SAR studies and further biological evaluation of this promising anticancer lead structure.[65]

RHIZOPODIN

Rhizopodin (**3**) is an architecturally complex macrocyclic polyketide first isolated in 1993 by Reichenbach and co-workers[66] from the myxobacterium *Myxococcus stipitatus*. By binding with and inhibiting actin polymerization, rhizopodin mediates potent antiproliferative activity as well as strong cytostatic effects against a range of cancer cell lines.[67] This selective interaction with actin also enabled its structural elucidation, with X-ray crystallographic studies of the bound rhizopodin–actin complex revealing an intriguing C_2-symmetric macrodiolide.[68] From a structural perspective, 14 of the 18 stereocenters are embedded in the 38-membered macrolide core, together with two oxazole rings and two diene motifs, with the remaining four stereocenters located on the two side chains.[69] The ornate architecture and promising anticancer profile of rhizopodin has rendered intensive research towards its total synthesis. Although several groups have reported the synthesis of various substructures,[70–74] there has only been two completed total syntheses of the target structure itself.[75–77]

Our proposed synthesis (Scheme 13) of rhizopodin (**3**) centered on structural simplification into the truncated monomer **69** and known side-chain fragment **70**.[78] This disconnection provided a degree of flexibility, with macrocycle formation possible via direct or sequential esterification, followed by bidirectional aldol coupling with ketone **70** to incorporate the requisite side chain(s). Oxazole formation was envisaged via amide bond formation between C14-C22 acid **71** and C8-C13 amino alcohol **72** followed by dehydration, while diene installation was proposed using a Stille coupling of vinyl iodide **73** and a suitable C8 stannane.

As is often the case with complex polyketide synthesis, the strategic incorporation of orthogonal-protecting groups was of crucial importance. Initially, we envisaged incorporating PMB ethers to chemoselectively unmask the required alcohols for the macrolactonization and side-chain attachment. However, we found that an oxidative PMB ether cleavage using dichloro-5,6-dicyanobenzoquinone resulted in the concomitant oxidation of the C5 allylic methyl ether, with alternative Lewis acidic cleavage degrading our advanced intermediates.[77] As such, we opted for a carefully selected combination of silyl-protecting groups. Notably, attempts at deprotecting the C16-OTBS ethers in the endgame resulted solely in eliminated product. Frustratingly also, attempts at deprotecting a primary C22-OTIPS ether to allow side-chain installation, in the presence of a secondary C16-OTES ether, resulted in simultaneous cleavage of both silyl groups. These difficulties ultimately forced us to opt for a riskier gamut of silyl-protecting groups in acid **71** and aldehyde **73** (*vide infra*).

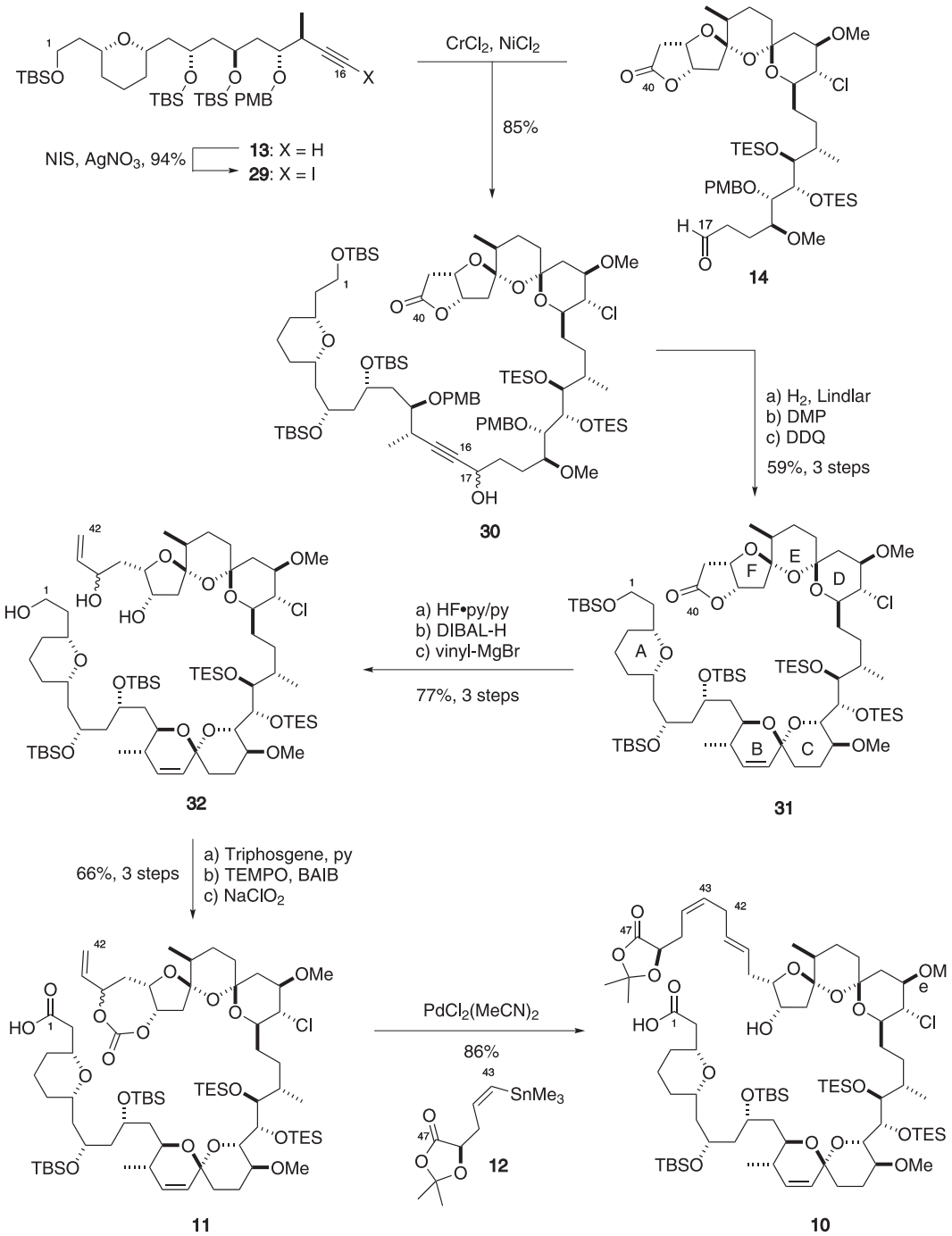

Scheme 6 Synthesis of the full C1-C47 carbon and oxygen skeleton of spirastrellolide A methyl ester **10**.

Synthesis of the C14-C22 carboxylic acid **71** commenced with a Brown allylation onto Roche ester-derived aldehyde **74** (Scheme 14a).[79] The remaining stereocenters in this fragment were generated first via a Mukaiyama aldol reaction between aldehyde **75** and silyl ketene acetal **76**, setting up the C18 stereocenter, and a subsequent diastereoselective reduction[80] of the cyclic ketone after methanolysis of dioxinone **77**. From β-hydroxylactone **78**, subsequent protections and oxidation afforded the C14-C22 acid **71**. The amino alcohol coupling partner **72** required for the oxazole formation was formed from propargyl alcohol **79** (Scheme 14b). A Sharpless asymmetric epoxidation (yielding epoxide **80**)[81,82] followed by amidation and regioselective epoxide opening gave oxazoline **81**. A final sequence of methylation and hydrolysis then delivered the amino alcohol **72**.

The final C1-C7 fragment **73** required for the macrocycle was obtained by an enantioselective Mukaiyama aldol reaction between aldehyde **82** and Chan's diene (**83**) (Scheme 14c).[83,84] Subsequent methanolysis of dioxinone **84** followed by a Narasaka reduction[85] generated the free diol. Protecting group manipulations and a final methylation of the free C5-OH then afforded the required Stille coupling partner **73**.

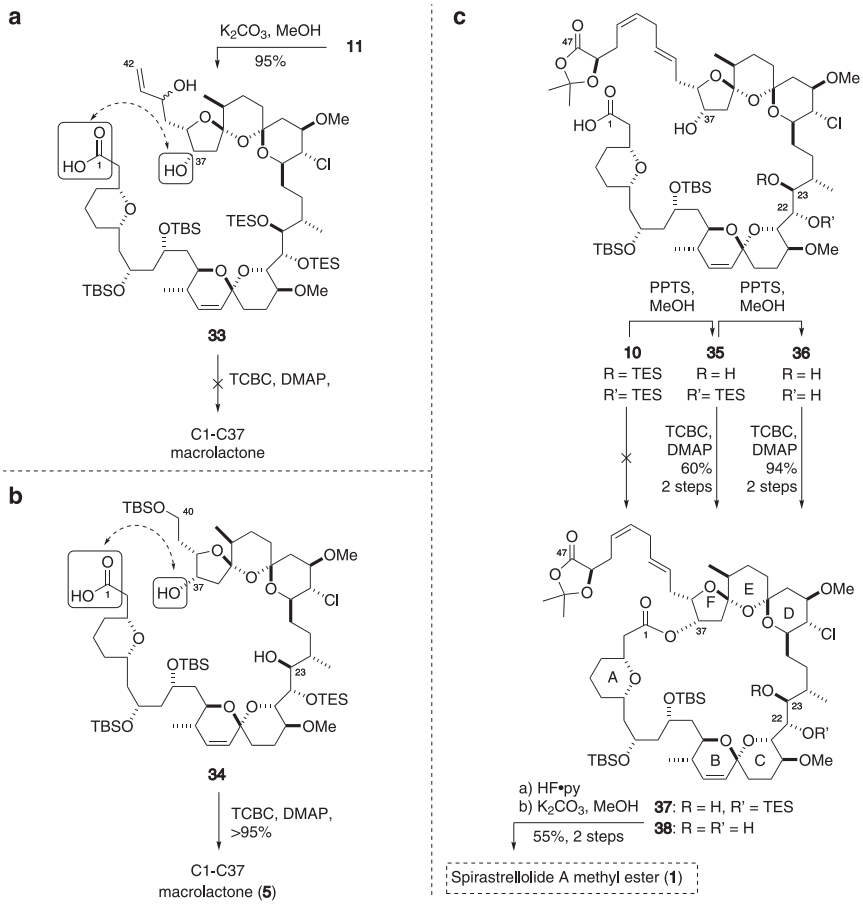

Scheme 7 (**a**) Truncated *seco*-acid **33** failed to macrocyclize when subjected to established macrolactonization conditions. (**b**) Macrocyclization conditions in our first-generation synthesis. (**c**) Endgame and total synthesis of spirastrellolide A methyl ester (**1**).

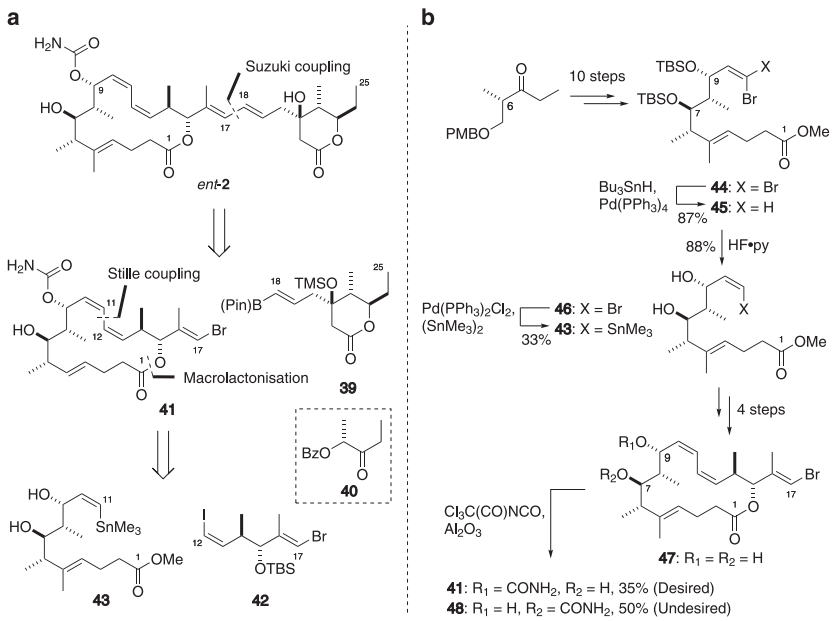

Scheme 8 (**a**) Initial approach towards leiodermatolide (*ent*-**2**). (**b**) Summary of our first-generation synthesis towards the C1-C17 macrocycle **41**.

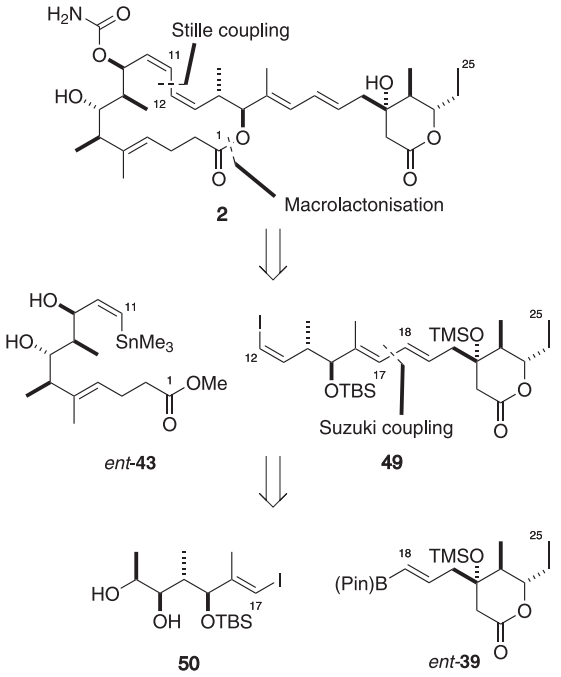

Scheme 9 Revised retrosynthesis for leiodermatolide (**2**).

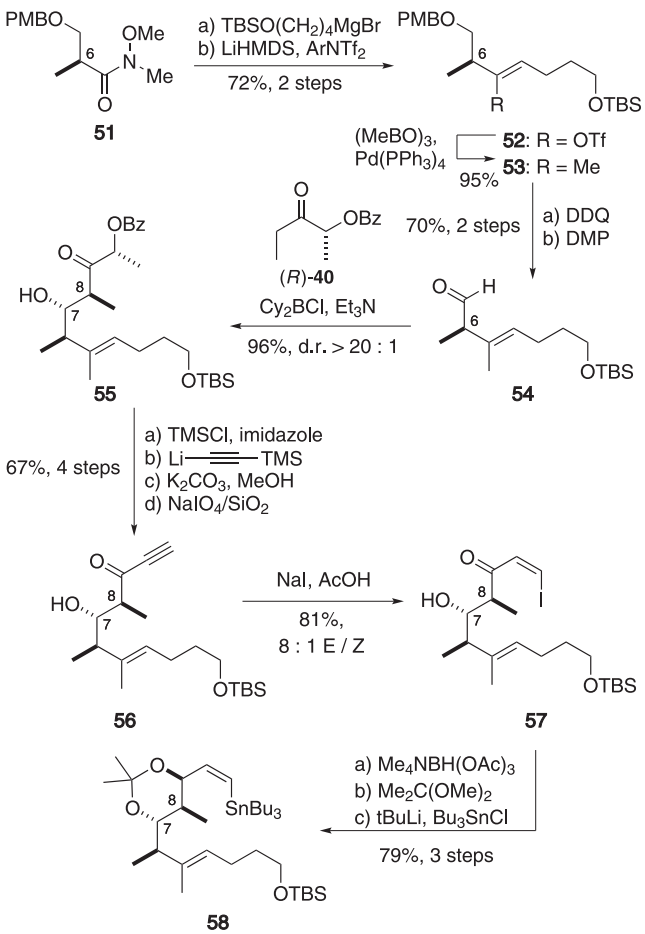

Scheme 10 Synthesis of the C1-C11 vinyl stannane **58**.

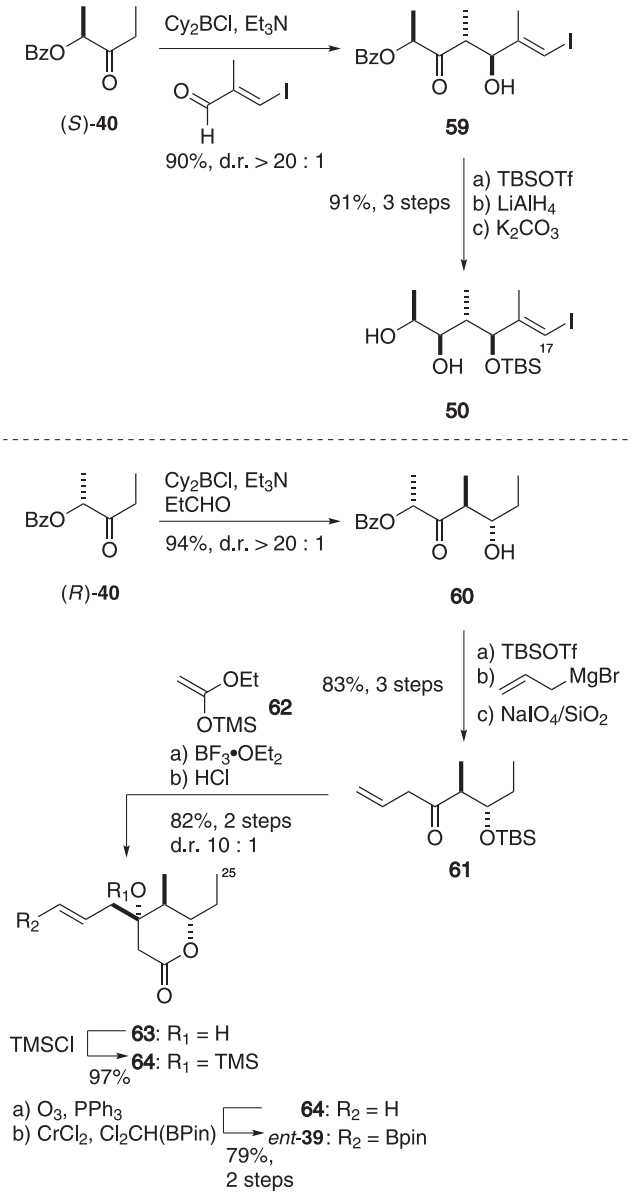

Scheme 11 Synthesis of the C12-C17 vinyl iodide **50** and C18-C25 δ-lactone *ent*-**39**.

Fragment assembly commenced with an amide bond formation between carboxylic acid **71** and amino alcohol **72** (Scheme 15). Using modified Robinson-Gabriel conditions developed by Wipf and Graham,[86] oxazole **85** was formed cleanly. Subsequent stannylation afforded vinyl stannane **86**, which was coupled with vinyl iodide **73** via a Stille cross-coupling[63] to give the truncated monomer in anticipation for the key macrocyclization step. At this stage, we discovered that a series of oxidation state adjustments and protecting group manipulations were critical for the success of the macrocycle formation. While conditions required for methyl ester hydrolysis concomitantly unmasked the required C18-OH, Yamaguchi macrolactonization conditions[39] disappointingly afforded a mixture of oligomers, primarily corresponding to the monomeric truncate. As such, we were forced to adopt a stepwise approach to access both coupling partners for the macrolactonization. A controlled reduction to the aldehyde **87** therefore was performed, meaning that this key intermediate could be subjected to either a controlled

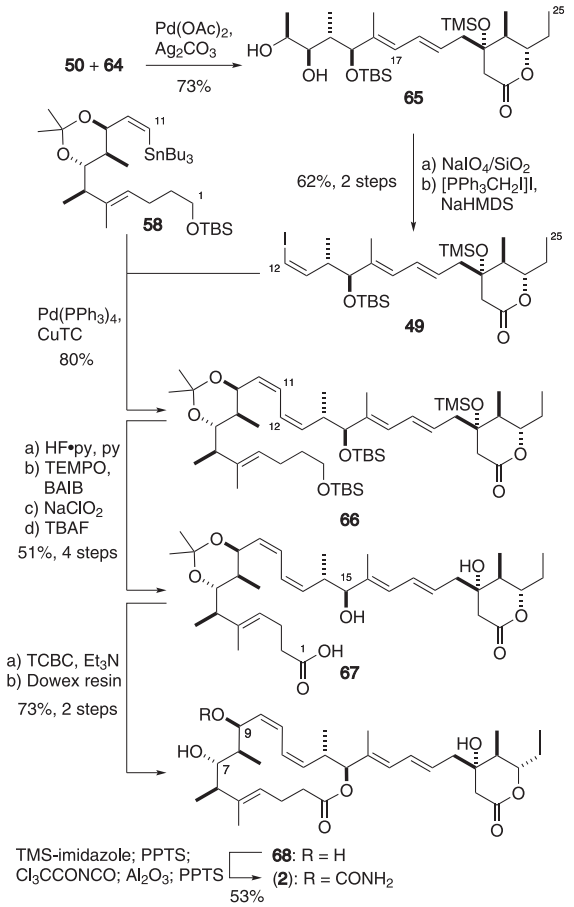

Scheme 12 Fragment union and completion of (–)-leiodermatolide (**2**).

C18-OTMS desilylation (**88**) or a Pinnick oxidation to afford *seco*-acid **89**.

Following these maneuvers, a selective esterification between alcohol **88** and *seco*-acid **89** served to complete the linear carbon skeleton in **90** (Scheme 16). This was followed by a similar sequence of desilylation, oxidation and macrolactonization to close the required macrocycle **91**. The C_2-symmetry of the molecule presented the opportunity of performing a bidirectional side-chain installation in the endgame. This required a selective C22-22′ primary TBS ether cleavage, a capricious operation owing to the presence of multiple secondary silyl-protecting groups of similar lability. In the end, carefully controlled exposure of the protected macrocycle **91** to HF/py selectively afforded the C22/22′ diol **92** which, following oxidation, underwent a double boron-mediated aldol addition with ketone **70**.[78] Drawing from our reidispongiolide synthesis,[78] a sequence involving a controlled dehydration,[87] followed by a conjugate reduction and global deprotection concluded our synthesis of rhizopodin (**3**) in 29 steps in 0.2% overall yield.[77] The eventual success of this project required judicious fine-tuning of the protecting group strategy and redox steps, emphasizing the need for perseverance based on a flexible synthesis plan.

CHIVOSAZOLE F

Following their discovery of rhizopodin, Reichenbach and co-workers[88] and Höfle and co-workers[89] reported the isolation of chivosazoles A-F from the myxobacterium *Sorangium cellulosum* in 1995. The chivosazoles are a structurally unprecedented class of polyene macrolides, with each member of the family differing in terms of the substitution at C11 and C20. Notably, the chivosazole family displayed potent inhibitory activity against filamentous fungi, yeast and a panel of human cancer cell lines. This bioactivity stems from its selective inhibition of actin polymerization. Intriguingly, the lack of structural homology to other known actin binders suggests that

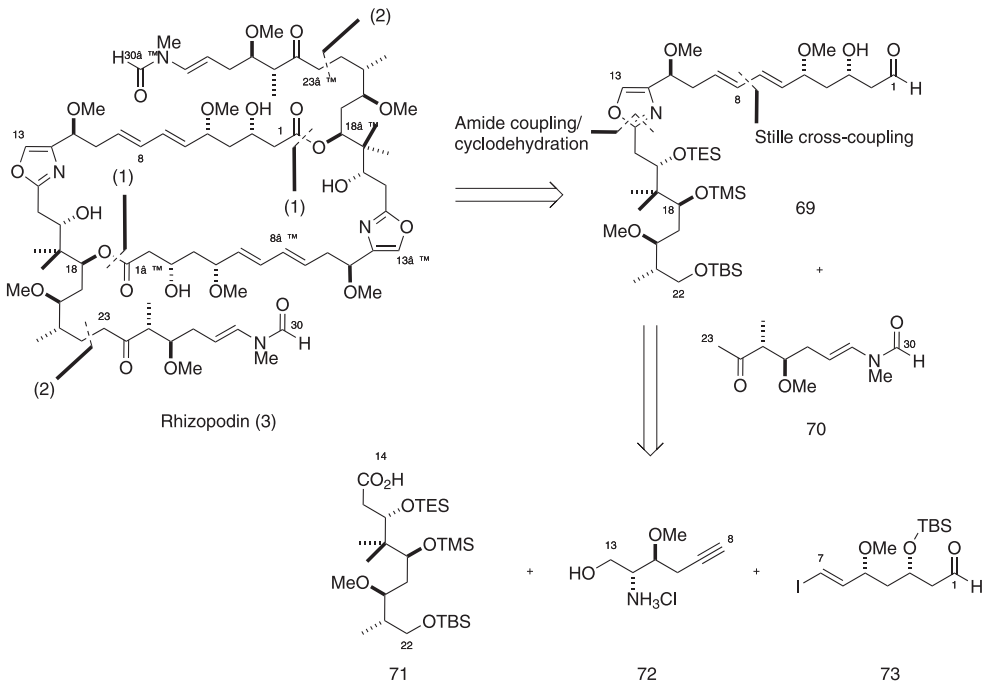

Scheme 13 Retrosynthetic analysis of rhizopodin (**3**). Disconnection (1) refers to an esterification/macrolactonization, and disconnection (2) refers to an aldol/dehydration/reduction sequence.

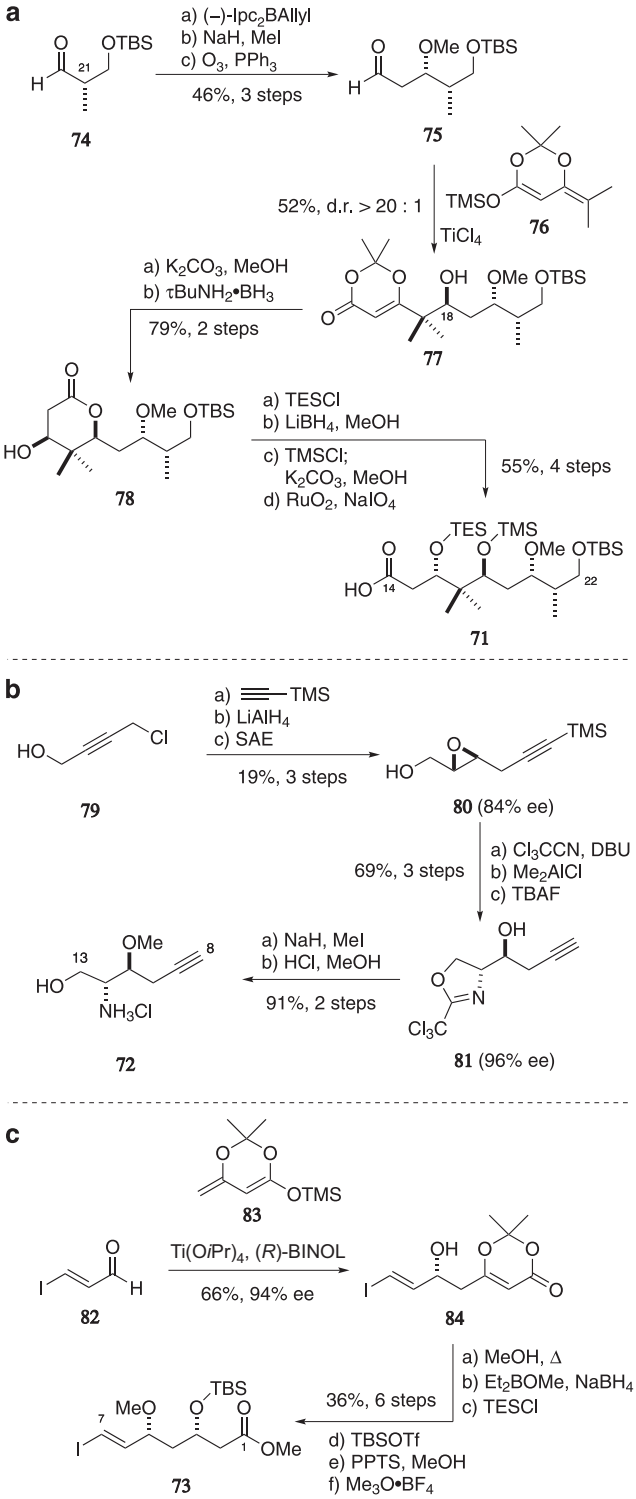

Scheme 14 (**a**) Synthesis of the C14-C22 carboxylic acid **71**. (**b**) Synthesis of the C8-C13 amino alcohol **72**. (**c**) Synthesis of the C1-C7 vinyl iodide **73**.

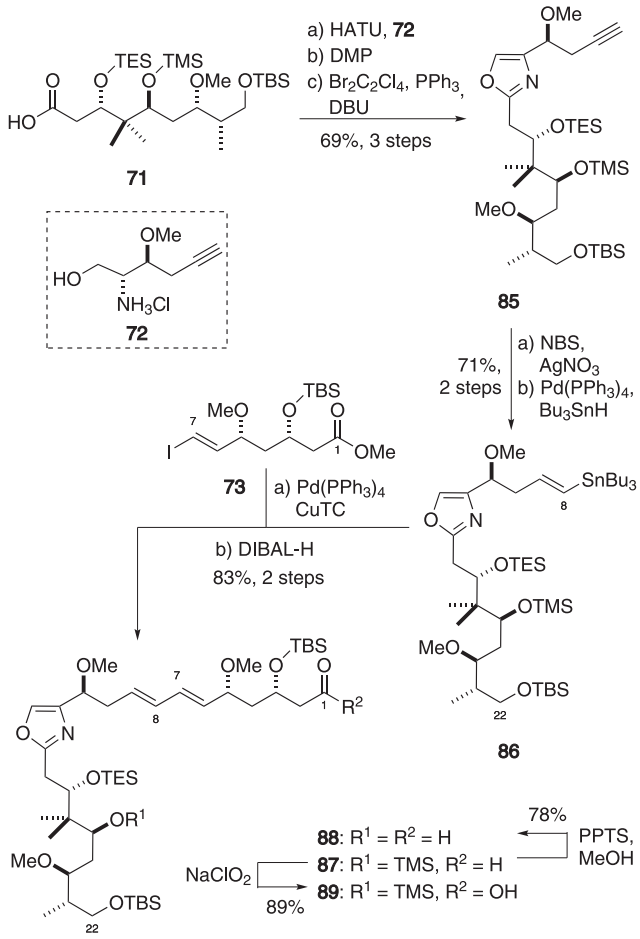

Scheme 15 Synthesis of the truncated C1-C22 monomers.

the chivosazoles may have a distinct mode of action.[90,91] What ignited our interest in the chivosazoles as a synthetic target was their astounding array of structural features (Scheme 17). Specifically, all congeners as typified by chivosazole F (**4**) possess a 31-membered macrolactone, containing 10 stereocenters and an oxazole moiety. However, the most impressive feature is the set of conjugated polyenes with alternating geometry in the macrocycle: a (*Z*,*E*,*Z*,*E*)-C2-C9 tetraene, a (*Z*,*E*)-C12-C15 diene and an (*E*,*E*,*Z*)-C23-C28 triene regions.[92] These polyene regions demanded careful handling of sensitive late-stage intermediates and mild reaction conditions, necessary to suppress both potential olefin isomerization and degradation pathways. Perhaps as a reflection of the challenges imposed by this demanding target, only two total syntheses of chivosazole F (**4**), including our approach described below, have been reported to date.[93,94]

Our synthetic approach needed to address the delicate nature of the chivosazole structure; in particular, the isomerization-prone (2*Z*,4*E*,6*Z*,8*E*)-tetraene. Therefore, we sought to minimize the number of endgame transformations. To this end, we envisaged a highly convergent approach towards accessing the full carbon skeleton by using site-selective cross-couplings. This broadly disconnects the full carbon skeleton to reveal the C14-C35 northern hemisphere and the C1-C13 southern hemisphere of the natural product.

The success of this strategy crucially relied on the judicious choice of coupling handles and cross-coupling conditions. Building on initial intelligence gathering studies, we discovered that the Stille cross-coupling provided the most efficient means of fragment union. We also anticipated that a late-stage macrolactonization might generate the macrocycle. This analysis revealed four constituent fragments—the C1-C5 fragment **93**, the

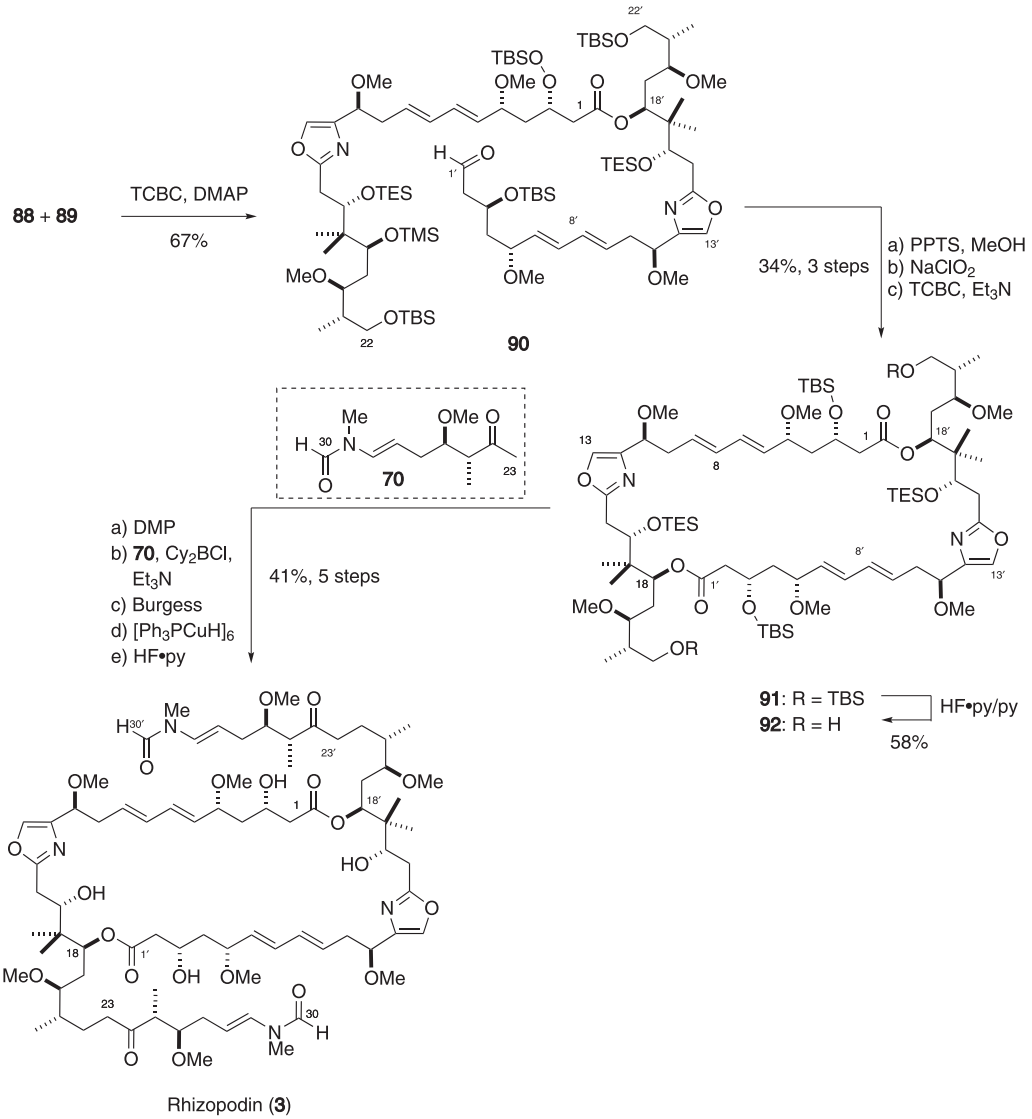

Scheme 16 Fragment union and completion of the total synthesis of rhizopodin (**3**).

C6-C13 fragment **94**, the C14-C26 fragment **95** and the C27-C35 fragment **96**.

Recognizing the 19,22-*syn* relationship, synthesis of the C14-C26 *bis*-halide linchpin commenced with an asymmetric boron-mediated aldol reaction from methyl ketone **97** and aldehyde **98**[95,96] to afford β-hydroxyketone **99** (Scheme 18a). This was then subjected to Evans–Tishchenko reduction[56] to establish the remaining stereocenter. The oxazoline ring was cyclized using diethylaminosulfur trifluoride[97] following amide formation from carboxylic acid **100** and amino alcohol **101**.[98] From oxazoline **102**, oxazole formation using MnO_2 proved incompatible with the pendant vinyl iodide functionality, suggesting that this oxidation step should be conducted postfragment assembly. Beginning from the ethyl ketone derivative **103** of (*S*)-Roche ester and known aldehyde **104**,[99,100] a boron-mediated aldol reaction[101] readily installed the C31 and C32 stereocenters in β-hydroxyketone **105**, with an Evans–Tishchenko reduction again used to set the final C30 stereocenter (Scheme 18b). A six-step sequence revealed aldehyde **106**, which was subjected to a Stork–Zhao olefination, deprotection and stannylation to afford the required stannane **96**.[49]

The C1-C13 southern hemisphere contains what is arguably the most delicate polyene region of the chivosazoles. A vinylogous Mukaiyama aldol reaction[102] between the chiral silyl ketene aminal **107** (derived from imide **108**) with aldehyde **109** forged the two stereocenters in the C7-C13 fragment **110** (Scheme 19).[103] Subsequent Stork–Zhao olefination of aldehyde **111** installed the terminal (6*Z*)-vinyl iodide in **112**, which then engaged in a site-selective Stille cross-coupling with stannane **93** to afford the C1-C13 southern hemisphere **113** in preparation for exploring the planned fragment coupling sequence.

With the two hemispheres in hand, we looked towards effecting the site-selective Stille coupling between the stannane **114** derived from **113** and *bis*-halide **102**. Unfortunately, not only did this fail to effect the required coupling, it also highlighted the propensity for the tetraenoate **114** to isomerize under Pd(0) conditions (Scheme 20a). Similarly, model studies investigating the esterification of **115** with vinyl stannane **116**, with the goal of effecting

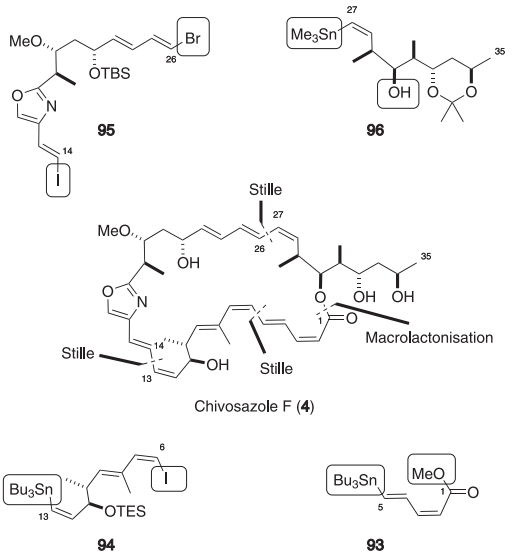

Scheme 17 Initial synthetic strategy towards chivosazole F (**4**) and the four proposed fragments.

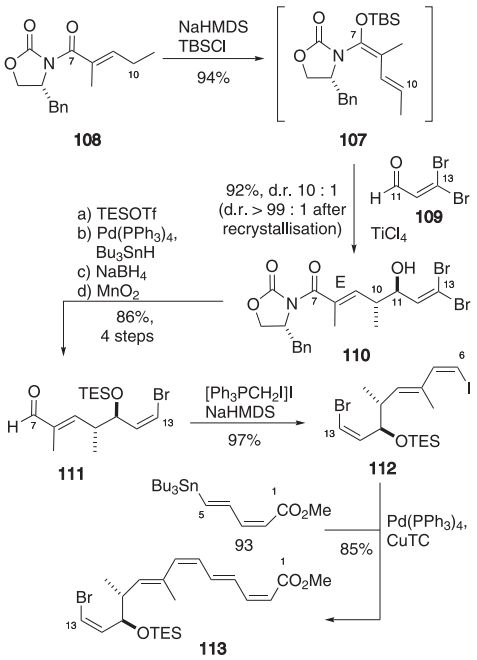

Scheme 19 Synthesis of the C1-C13 southern hemisphere fragment **113**.

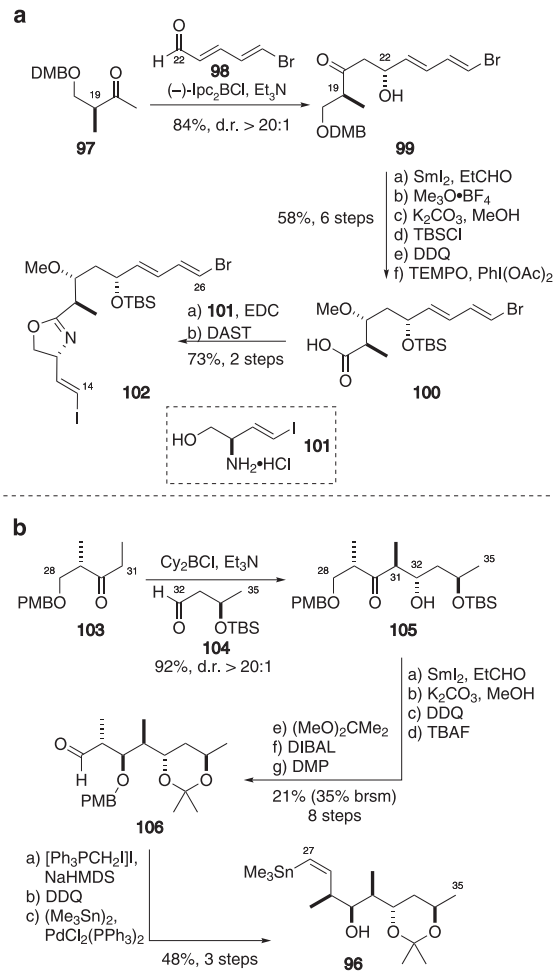

Scheme 18 (**a**) Synthesis of the C14-C26 *bis*-halide linchpin **102**. (**b**) Synthesis of the C27-C35 vinyl stannane **96**.

a macro-Stille ring closure, afforded the isomerized (2*E*,4*E*)-stannane **117** under Yamaguchi conditions (Scheme 20b). To avoid handling the isomerization-prone (2*Z*) olefin, we next investigated the possibility of achieving a late-stage macro-olefination with a pendant phosphonate ester at C30 in **118**. The revised synthesis of the southern hemisphere thus involved a Stille coupling with vinyl iodide **94** and stannane **120** (Scheme 20c).

Using optimized Stille cross-coupling conditions, and rationalizing chemoselective coupling on steric and electronic grounds, we were able to append C3-C5 stannane **119** onto the C6-C13 vinyl iodide **94** to yield the C1-C13 tetraene **120** (Scheme 21). Crucially, addition of $t\text{Bu}_3\text{P}$[104] was required to prevent isomerization of the (6*Z*)-alkene. These conditions also allowed for the successful site-selective formation of the C13-C14 bond between *bis*-halide **102** and vinyl stannane **120**, as well elaborating the resulting vinyl bromide **121** with the C27-C35 fragment **118** (derived from vinyl iodide **122**), with complete control of alkene geometry throughout the process. This success led us to ponder whether we could turn this into a one-pot process. Remarkably, with sequential addition of each fragment (i. **119**, ii. **94**, iii. **102** and iv. **118**), we were able to assemble the full carbon skeleton of the chivosazoles in **123** in one pot in 56% yield (82% per coupling step). At this advanced stage, the (4*E*,6*Z*,8*E*)-triene was found to be highly prone to isomerization on attempting to adjust the oxidation state at C3 ahead of the planned Horner–Wadsworth–Emmons-type macro-olefination. Furthermore, model studies on the planned Ando-olefination[105] gave poor control over the desired 2*Z* geometry. This series of disappointing and incredibly frustrating setbacks forced us to return to the drawing board.

The challenges imposed by the delicate triene necessitated us to reconfigure our choreography of fragment coupling to an end-stage macro-Stille cyclization (Scheme 22). Furthermore, to access the (2*Z*) geometry, an alternative olefination strategy was required. The

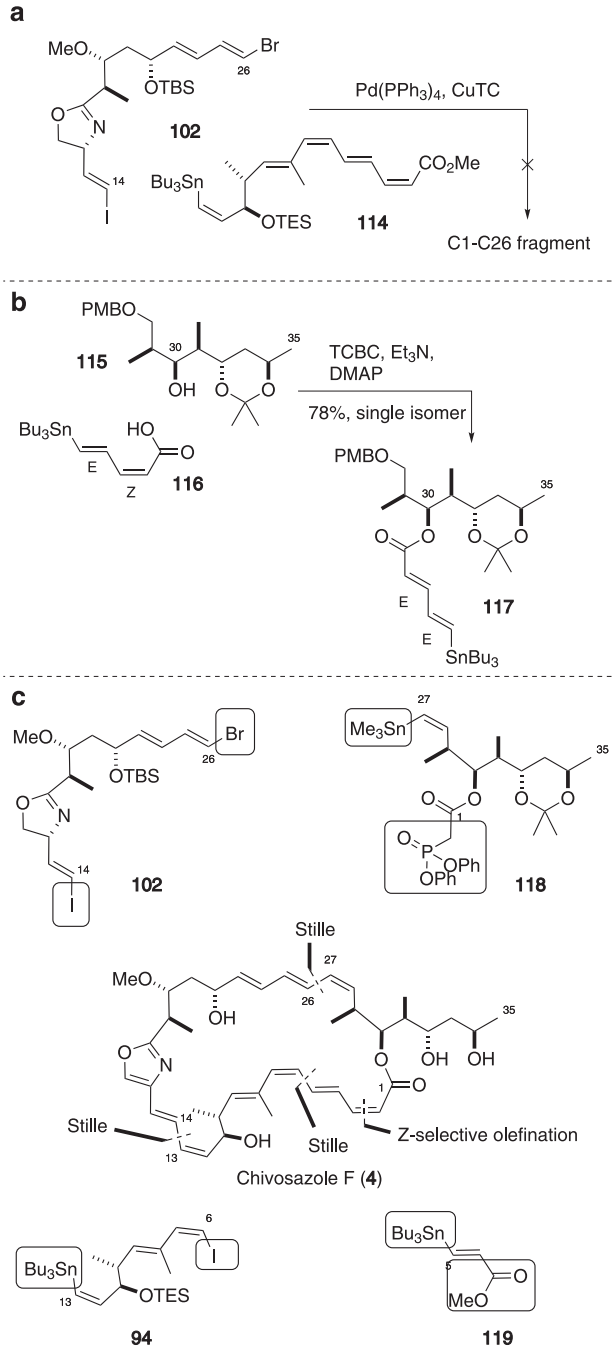

Scheme 20 (**a**) Initial attempts at fragment union under Stille conditions failed to deliver the product and resulted in isomerization of the tetraenoate. (**b**) Esterification of alcohol **115** to the C1-C5 acid **116** resulted in concomitant isomerization of the C2 olefin. (**c**) Our revised synthetic approach to chivosazole F (**4**).

anticipated lability of the target molecule also prompted us to switch from an acetonide to a silylene-protecting group for the 32,34-diol to facilitate a mild final deprotection. These alterations meant that our constituent fragments towards assembling **4** would involve a C3-C5 aldehyde **124**, a revised C7-C13 stannane **125** and a revised C27-C35 phosphonate **126**.

The revised C27-C35 phosphonate **126** was made from diol **127**,[94] an intermediate used in our previous routes. Building on the prior work, fragment coupling could be conducted in a stepwise manner (via the C7-C26 vinyl bromide **128**) or a one-pot process (i. **102** ii. **125** iii. **126**) to deliver efficiently the advanced fragment **129** (Scheme 23). Gratifyingly, using the Still–Gennari-type phosphonate afforded useful selectivities towards the desired 2*Z* geometry for the Horner–Wadsworth–Emmons olefination with aldehyde **124**.[106,107] At this stage, a double oxidation of the C7-OH and the oxazoline was carried out using MnO_2, notably accomplishing the challenging aromatization on a delicate advanced fragment. Subsequently, the resulting aldehyde **130** was elaborated via a Stork–Zhao olefination to furnish the full carbon skeleton and also the *seco* precursor for the ring-closing

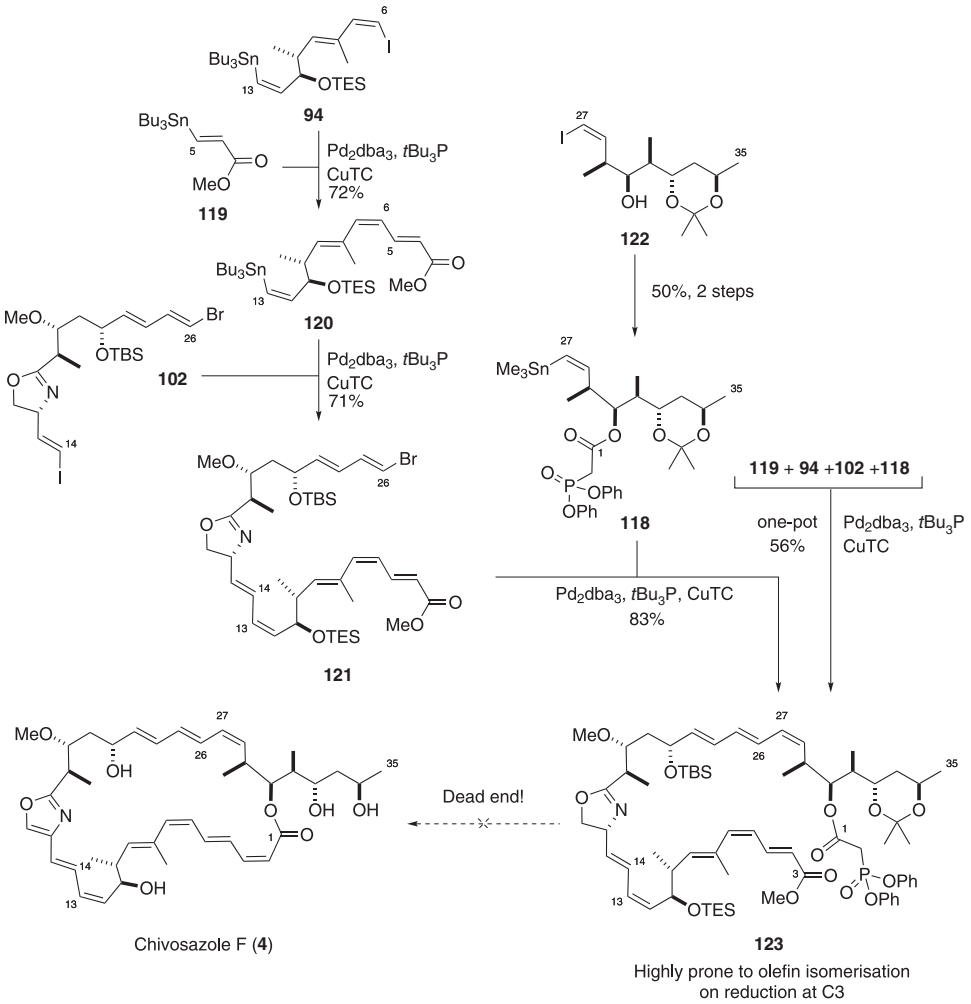

Scheme 21 Using the site-selective Stille coupling strategy to form the chivosazole backbone.

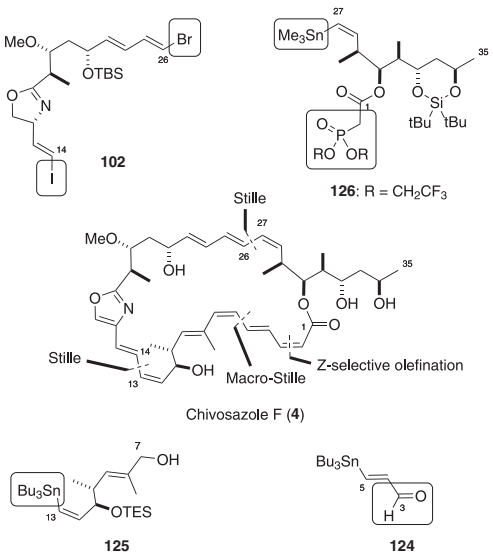

Scheme 22 Final strategy adopted towards the total synthesis of chivosazole F (**4**).

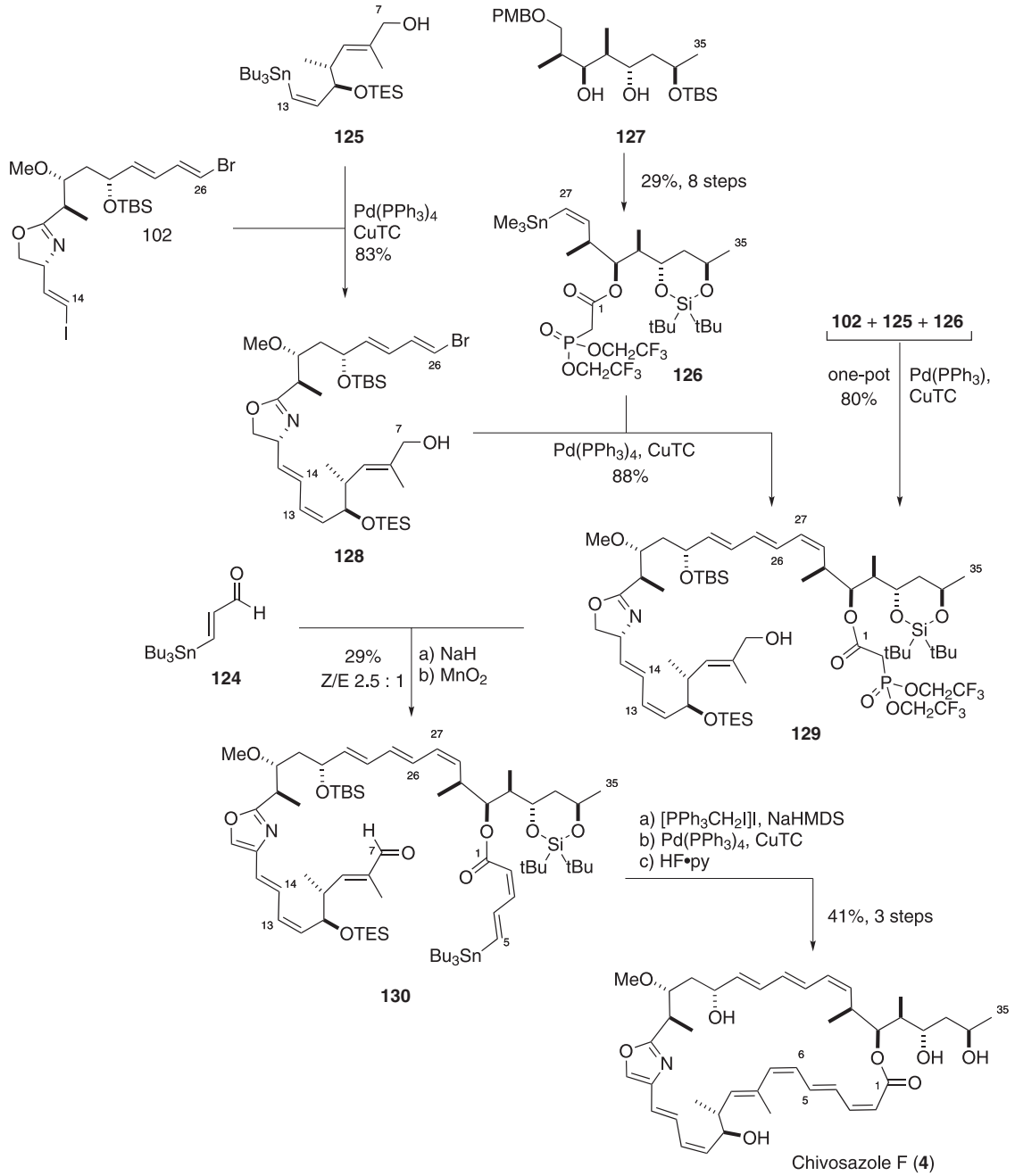

Scheme 23 Revised fragment coupling and completion of the total synthesis of chivosazole F (**4**).

intramolecular Stille reaction. To our delight, the critical macrocyclization delivered the protected natural product with complete retention of olefin geometry. A final global deprotection concluded our total synthesis of chivosazole F (**4**) in 20 steps and 2.5% overall yield. Our success in this arduous campaign hinged upon careful initial analysis and planning, which fortunately, allowed for a highly convergent approach and a succinct endgame sequence. While we recognized the potential lability of such advanced polyene fragments, we could not have anticipated the frustration it brought. In this case, it truly stressed the importance of a flexible, modular strategy and the ability to adapt the strategy as required.

CONCLUSIONS

Our recent synthetic endeavors towards these highly challenging classes of complex polyketides not only showcases the versatility of our group's aldol methodology but also highlights the trials and tribulations we overcame in a sustained campaign to achieve these enticing targets. In our total synthesis of spirastrellolide A methyl ester, we discovered that the subtle, unexpected structural effects imposed by distal-protecting groups proved to be highly consequential in the critical macrolactonization. Similarly, for rhizopodin, a carefully choreographed sequence of protecting group incorporation and selective deprotection, was pivotal to achieving the target. Our campaign towards leiodermatolide underlines the need

to reassess fragment coupling strategies when required. This is a common theme and important lesson—and was certainly a defining obstacle in our campaign towards chivosazole F. In the end, a carefully orchestrated sequence of fragment coupling steps proved to be vital for success.

In this account, the highlighted setbacks and accompanying explanations of strategy evolution serve to illuminate the unanticipated difficulties that can make or break a total synthesis. Overall, we are provided with a humbling reminder that despite continual advances in the field of chemical synthesis, there is still much to be learned from tackling a structurally complex natural product.

DEDICATION

Dedicated to Professor KC Nicolaou.

CONFLICT OF INTEREST

The authors declare no conflict of interest.

ACKNOWLEDGEMENTS

The work summarized in this review was carried out by generations of highly able students and postdocs at Cambridge, whose dedication, hard work and contributions are gratefully acknowledged. We thank the Woolf Fisher Trust (scholarship to NYSL) for support, Dr Alison Findlay for helpful discussions and a thorough review of the manuscript and the EPSRC UK National Mass Spectrometry Facility at Swansea University.

1 Newman, D. J. & Cragg, G. M. Marine natural products and related compounds in clinical and advanced preclinical trials. *J. Nat. Prod.* **67**, 1216–1238 (2004).
2 Norcross, R. D. & Paterson, I. Total synthesis of bioactive marine macrolides. *Chem. Rev.* **95**, 2041–2114 (1995).
3 Newman, D. J. & Cragg, G. M. Natural products as sources of new drugs from 1981 to 2014. *J. Nat. Prod.* **79**, 629–661 (2016).
4 Yeung, K.-S. & Paterson, I. Advances in the total synthesis of biologically important marine macrolides. *Chem. Rev.* **105**, 4237–4313 (2005).
5 Paterson, I. & Anderson, E. The renaissance of natural products as drug candidates. *Science* **310**, 451–453 (2005).
6 Dalby, S. M. & Paterson, I. Synthesis of polyketide natural products and analogs as promising anticancer agents. *Curr. Opin. Drug Discov. Dev.* **13**, 777–794 (2010).
7 Paterson, I. & Findlay, A. D. Recent advances in the total synthesis of polyketide natural products as promising anticancer agents. *Aust. J. Chem.* **62**, 624–638 (2009).
8 Kan, S. B. J., Ng, K. K.-H. & Paterson, I. The impact of the Mukaiyama aldol reaction in total synthesis. *Angew. Chem. Int. Ed.* **52**, 9097–9108 (2013).
9 Paterson, I. New methods and strategies for the stereocontrolled synthesis of polypropionate-derived natural products. *Pure Appl. Chem.* **64**, 1821–1830 (1992).
10 Williams, D. E., Roberge, M., Van Soest, R. & Andersen, R. J. Spirastrellolide A, an antimitotic macrolide isolated from the Caribbean marine sponge *Spirastrella coccinea*. *J. Am. Chem. Soc.* **125**, 5296–5297 (2003).
11 Paterson, I., Maltas, P. & Anderson, E. A. Total synthesis of (+)-spirastrellolide A methyl ester: challenges and discoveries. *Pure Appl. Chem.* **85**, 1133–1147 (2013).
12 Williams, D. E. *et al.* Spirastrellolide A: revised structure, progress toward the relative configuration, and inhibition of protein phosphatase 2A. *Org. Lett.* **6**, 2607–2610 (2004).
13 Warabi, K., Williams, D. E., Patrick, B. O., Roberge, M. & Andersen, R. J. Spirastrellolide B reveals the absolute configuration of the spirastrellolide macrolide core. *J. Am. Chem. Soc.* **129**, 508–509 (2007).
14 Williams, D. E. *et al.* Spirastrellolides C to G: macrolides obtained from the marine sponge *Spirastrella coccinea*. *J. Org. Chem.* **72**, 9842–9845 (2007).
15 Paterson, I. & Dalby, S. M. Synthesis and stereochemical determination of the spirastrellolides. *Nat. Prod. Rep.* **26**, 865–873 (2009).
16 Vintonyak, V. V., Antonchick, A. P., Rauh, D. & Waldmann, H. The therapeutic potential of phosphatase inhibitors. *Curr. Opin. Chem. Biol.* **13**, 272–283 (2009).
17 O'Neil, G. W. *et al.* Total synthesis of spirastrellolide F methyl ester—part 1: strategic considerations and revised approach to the southern hemisphere. *Angew. Chem. Int. Ed.* **48**, 9940–9945 (2009).
18 Benson, S. *et al.* Total synthesis of spirastrellolide F methyl ester—part 2: macrocyclization and completion of the synthesis. *Angew. Chem. Int. Ed.* **48**, 9946–9950 (2009).
19 Benson, S. *et al.* Second-generation total synthesis of spirastrellolide F methyl ester: the alkyne route. *Angew. Chem. Int. Ed.* **50**, 8739–8744 (2011).
20 Arlt, A., Benson, S., Schulthoff, S., Gabor, B. & Fürstner, A. A total synthesis of spirastrellolide A methyl ester. *Chem. Eur. J.* **19**, 3596–3608 (2013).
21 Paterson, I. *et al.* Total synthesis of spirastrellolide A methyl ester—Part 1: synthesis of an advanced C17–C40 bis-spiroacetal Subunit. *Angew. Chem. Int. Ed.* **47**, 3016–3020 (2008).
22 Paterson, I. *et al.* Total synthesis of spirastrellolide A methyl ester—part 2: subunit union and completion of the synthesis. *Angew. Chem. Int. Ed.* **47**, 3021–3025 (2008).
23 Paterson, I., Maltas, P., Dalby, S. M., Lim, J. H. & Anderson, E. A. A second-generation total synthesis of spirastrellolide A methyl ester. *Angew. Chem. Int. Ed.* **51**, 2749–2753 (2012).
24 Paterson, I. *et al.* The stereocontrolled total synthesis of spirastrellolide A methyl ester. Expedient construction of the key fragments. *Org. Biomol. Chem.* **10**, 5861–5872 (2012).
25 Paterson, I. *et al.* Progress toward a total synthesis of spirastrellolide A. *Pure Appl. Chem.* **79**, 667–676 (2007).
26 Paterson, I., Anderson, E. A., Dalby, S. M., Lim, J. H. & Maltas, P. The stereocontrolled total synthesis of spirastrellolide A methyl ester. Fragment coupling studies and completion of the synthesis. *Org. Biomol. Chem.* **10**, 5873–5886 (2012).
27 Chatterjee, A. K., Choi, T.-L., Sanders, D. P. & Grubbs, R. H. A general model for selectivity in olefin cross metathesis. *J. Am. Chem. Soc.* **125**, 11360–11370 (2003).
28 Nicolaou, K. C., Bulger, P. G. & Sarlah, D. Metathesis reactions in total synthesis. *Angew. Chem. Int. Ed.* **44**, 4490–4527 (2005).
29 Miyaura, N. & Suzuki, A. Palladium-catalyzed cross-coupling reactions of organoboron compounds. *Chem. Rev.* **95**, 2457–2483 (1995).
30 Paterson, I. *et al.* Synthesis of the DEF-bis-spiroacetal of spirastrellolide A exploiting a double asymmetric dihydroxylation/spiroacetalisation strategy. *Chem. Commun.* 4186–4188 (2006).
31 Paterson, I., Anderson, E. A., Dalby, S. M. & Loiseleur, O. Toward the synthesis of spirastrellolide A: construction of a tetracyclic C26-C40 subunit containing the DEF-bis-spiroacetal. *Org. Lett.* **7**, 4121–4124 (2005).
32 Shaojing, H., Jayaraman, S. & Oehlschlager, A. C. Diastereo- and enantioselective synthesis of syn-α-vinylchlorohydrins and *cis*-vinylepoxides. *J. Org. Chem.* **61**, 7513–7520 (1996).
33 Paterson, I., Wallace, D. J. & Cowden, C. J. Polyketide synthesis using the boron-mediated, anti-aldol reactions of lactate-derived ketones: total synthesis of (−)-ACRL toxin IIIB. *Synthesis* **1998**, 639–652 (1998).
34 Kolb, H. C., VanNieuwenhze, M. S. & Sharpless, K. B. Catalytic asymmetric dihydroxylation. *Chem. Rev.* **94**, 2483–2547 (1994).
35 Paterson, I., Anderson, E. A., Dalby, S. M. & Loiseleur, O. Toward the synthesis of spirastrellolide A: construction of two C1-C25 diastereomers containing the BC-spiroacetal. *Org. Lett.* **7**, 4125–4128 (2005).
36 Chemler, S. R., Trauner, D. & Danishefsky, S. J. The B-alkyl Suzuki–Miyaura cross-coupling reaction: development, mechanistic study, and applications in natural product synthesis. *Angew. Chem. Int. Ed.* **40**, 4544–4568 (2001).
37 Takai, K., Kimura, K., Kuroda, T., Hiyama, T. & Nozaki, H. Selective Grignard-type carbonyl addition of alkenyl halides mediated by chromium(II) chloride. *Tetrahedron Lett.* **24**, 5281–5284 (1983).
38 Jin, H., Uenishi, J., Christ, W. J. & Kishi, Y. Catalytic effect of nickel(II) chloride and palladium(II) acetate on chromium(II)-mediated coupling reaction of iodo olefins with aldehydes. *J. Am. Chem. Soc.* **108**, 5644–5646 (1986).
39 Inanaga, J., Hirata, K., Saeki, H., Katsuki, T. & Yamaguchi, M. A rapid esterification by means of mixed anhydride and its application to large-ring lactonization. *Bull. Chem. Soc. Jpn* **52**, 1989–1993 (1979).
40 Shiina, I., Kubota, M., Oshiumi, H. & Hashizume, M. An effective use of benzoic anhydride and its derivatives for the synthesis of carboxylic esters and lactones: a powerful and convenient mixed anhydride method promoted by basic catalysts. *J. Org. Chem.* **69**, 1822–1830 (2004).
41 Wright, A. E., Reed, J. K., Roberts, J. & Longley, R. E. Antiproliferative activity of the leiodermatolide class of macrolides. U.S. Pat. Appl. Publ. (USA) US2008033035.
42 Paterson, I. *et al.* Leiodermatolide, a potent antimitotic macrolide from the marine sponge Leiodermatium sp. *Angew. Chem. Int. Ed.* **50**, 3219–3223 (2011).
43 Smith, S. G. & Goodman, J. M. Assigning stereochemistry to single diastereoisomers by GIAO NMR calculation: the DP4 probability. *J. Am. Chem. Soc.* **132**, 12946–12959 (2010).
44 Reiss, A. & Maier, M. E. Toward leiodermatolide: synthesis of the core structure. *Org. Lett.* **18**, 3146–3149 (2016).
45 Rink, C., Navickas, V. & Maier, M. E. An approach to the core structure of leiodermatolide. *Org. Lett.* **13**, 2334–2337 (2011).
46 Mailhol, D. *et al.* Synthesis, molecular editing, and biological assessment of the potent cytotoxin leiodermatolide. *J. Am. Chem. Soc.* **136**, 15719–15729 (2014).
47 Willwacher, J., Kausch-Busies, N. & Fürstner, A. Divergent total synthesis of the antimitotic agent leiodermatolide. *Angew. Chem. Int. Ed.* **51**, 12041–12046 (2012).
48 Paterson, I., Paquet, T. & Dalby, S. M. Synthesis of the macrocyclic core of leiodermatolide. *Org. Lett.* **13**, 4398–4401 (2011).
49 Wulff, W. D. *et al.* A regioselective entry to vinyl lithiums from unsymmetrical ketones via enol triflates. *J. Org. Chem.* **51**, 277–279 (1986).
50 Kočovský, P. Carbamates : a method of synthesis and some synthetic applications. *Tetrahedron Lett.* **27**, 5521–5524 (1986).
51 Paterson, I. & Williams, S. Strategy evolution in the total synthesis of (−)-leiodermatolide. *Isr. J. Chem.* **57**, 192–201 (2017).

52 Comins, D. L. & Dehghani, A. Pyridine-derived triflating reagents: an improved preparation of vinyl triflates from metallo enolates. *Tetrahedron Lett.* **33**, 6299–6302 (1992).
53 Gray, M., Andrews, I. P., Hook, D. F., Kitteringham, J. & Voyle, M. Practical methylation of aryl halides by Suzuki–Miyaura coupling. *Tetrahedron Lett.* **41**, 6237–6240 (2000).
54 Paterson, I., Wallace, D. J. & Velázquez, S. M. Studies in polypropionate synthesis: high π-face selectivity in syn and anti aldol reactions of chiral boron enolates of lactate-derived ketones. *Tetrahedron Lett.* **35**, 9083–9086 (1994).
55 Paterson, I. & Wallace, D. J. Manipulation of the aldol adducts from lactate-derived ketones. A versatile chiral auxiliary for the asymmetric synthesis of β-hydroxy carbonyl compounds. *Tetrahedron Lett.* **35**, 9087–9090 (1994).
56 Evans, D. A. & Hoveyda, A. H. Samarium-catalyzed intramolecular Tishchenko reduction of β-hydroxy ketones. A stereoselective approach to the synthesis of differentiated anti 1,3-diol monoesters. *J. Am. Chem. Soc.* **112**, 6447–6449 (1990).
57 Evans, D. A., Chapman, K. T. & Carreira, E. M. Directed reduction of β-hydroxy ketones employing tetramethylammonium triacetoxyborohydride. *J. Am. Chem. Soc.* **110**, 3560–3578 (1988).
58 Taniguchi, M., Kobayashi, S., Nakagawa, M., Hino, T. & Kishi, Y. β-Halovinyl ketones: synthesis from acetylenic ketones. *Tetrahedron Lett.* **27**, 4763–4766 (1986).
59 Paterson, I., Ng, K. K.-H., Williams, S., Millican, D. C. & Dalby, S. M. Total synthesis of the antimitotic marine macrolide (−)-leiodermatolide. *Angew. Chem. Int. Ed.* **53**, 2692–2695 (2014).
60 Mukaiyama, T., Banno, K. & Narasaka, K. New cross-aldol reactions. Reactions of silyl enol ethers with carbonyl compounds activated by titanium tetrachloride. *J. Am. Chem. Soc.* **96**, 7503–7509 (1974).
61 Evans, D. A., Dart, M. J., Duffy, J. L., Yang, M. G. & Livingston, A. B. Diastereoselective aldol and allylstannane addition reactions. The merged stereochemical impact of α and β aldehyde substituents. *J. Am. Chem. Soc.* **117**, 6619–6620 (1995).
62 Jeffery, T. *et al.* Palladium-catalysed reaction of vinylic halides with allylic alcohols: a highly chemo-, regio- and stereo-controlled synthesis of conjugated dienols. *J. Chem. Soc. Chem. Commun.* 324–325 (1991).
63 Fürstner, A. *et al.* A versatile protocol for Stille–Migita cross coupling reactions. *Chem. Commun.* 2873–2875 (2008).
64 Stille, J. K. & Groh, B. L. Stereospecific cross-coupling of vinyl halides with vinyl tin reagents catalyzed by palladium. *J. Am. Chem. Soc.* **109**, 813–817 (1987).
65 Guzmán, E. A. *et al.* Leiodermatolide, a novel marine natural product, has potent cytotoxic and antimitotic activity against cancer cells, appears to affect microtubule dynamics, and exhibits antitumor activity. *Int. J. Cancer* **139**, 2116–2126 (2016).
66 Sasse, F., Steinmetz, H., Höfle, G. & Reichenbach, H. Rhizopodin, a new compound from *Myxococcus stipitatus* (myxobacteria) causes formation of rhizopodia-like structures in animal cell cultures. Production, isolation, physico-chemical and biological properties. *J. Antibiot. (Tokyo)* **46**, 741–748 (1993).
67 Gronewold, T. M. A., Sasse, F., Lünsdorf, H. & Reichenbach, H. Effects of rhizopodin and latrunculin B on the morphology and on the actin cytoskeleton of mammalian cells. *Cell Tissue Res.* **295**, 121–129 (1999).
68 Jansen, R. *et al.* Isolation and structure revision of the actin-binding macrolide rhizopodin from *Myxococcus stipitatus* (Myxobacteria). *Tetrahedron Lett.* **49**, 5796–5799 (2008).
69 Horstmann, N. & Menche, D. Configurational assignment of rhizopodin, an actin-binding macrolide from the myxobacterium *Myxococcus stipitatus*. *Chem. Commun.* 5173–5175 (2008).
70 Pulukuri, K. K. & Chakraborty, T. K. Stereoselective synthesis of the monomeric unit of actin binding macrolide rhizopodin. *Org. Lett.* **14**, 2858–2861 (2012).
71 Chen, Z., Song, L., Xu, Z. & Ye, T. Synthesis of the C9 – C23 (C9′ – C23′) fragment of the dimeric natural product rhizopodin. *Org. Lett.* **12**, 2036–2039 (2010).
72 Nicolaou, K. C. *et al.* Total synthesis and biological evaluation of monorhizopodin and 16-epi-monorhizopodin. *Angew. Chem. Int. Ed.* **50**, 1139–1144 (2011).
73 Pulukuri, K. K. & Chakraborty, T. K. Formal synthesis of actin binding macrolide rhizopodin. *Org. Lett.* **16**, 2284–2287 (2014).
74 Bender, T., Loits, D., White, J. M. & Rizzacasa, M. A. Synthesis of the C1–C18 fragment of rhizopodin: late-state introduction of the oxazole. *Org. Lett.* **16**, 1450–1453 (2014).
75 Dieckmann, M. *et al.* Total synthesis of rhizopodin. *Angew. Chem. Int. Ed.* **51**, 5667–5670 (2012).
76 Kretschmer, M. *et al.* Modular total synthesis of rhizopodin: a highly potent G-actin dimerizing macrolide. *Chem. Eur. J* **19**, 15993–16018 (2013).
77 Dalby, S. M., Goodwin-Tindall, J. & Paterson, I. Total synthesis of (−)-rhizopodin. *Angew. Chem. Int. Ed.* **52**, 6517–6521 (2013).
78 Paterson, I. *et al.* Total synthesis of (−)-reidispongiolide A, an actin-targeting macrolide isolated from the marine sponge *Reidispongia coerulea*. *Chem. Asian J.* **3**, 367–387 (2008).
79 Jadhav, P. K., Bhat, K. S., Perumal, P. T. & Brown, H. C. Chiral synthesis via organoboranes. 6. Asymmetric allylboration via chiral allyldialkylboranes. Synthesis of homoallylic alcohols with exceptionally high enantiomeric excess. *J. Org. Chem.* **51**, 432–439 (1986).
80 Hinterding, K., Singhanat, S. & Oberer, L. Stereoselective synthesis of polyketide fragments using a novel intramolecular Claisen-like condensation/reduction sequence. *Tetrahedron Lett.* **42**, 8463–8465 (2001).
81 Hanson, R. M. & Sharpless, K. B. Procedure for the catalytic asymmetric epoxidation of allylic alcohols in the presence of molecular sieves. *J. Org. Chem.* **51**, 1922–1925 (1986).
82 Gao, Y. *et al.* Catalytic asymmetric epoxidation and kinetic resolution: modified procedures including in situ derivatization. *J. Am. Chem. Soc.* **109**, 5765–5780 (1987).
83 De Rosa, M., Soriente, A. & Scettri, A. Enantioselective aldol condensation of O-silyl dienolates to aldehydes mediated by chiral BINOL–titanium complexes. *Tetrahedron: Asymmetry* **11**, 3187–3195 (2000).
84 Paterson, I., Davies, R. D. M., Heimann, A. C., Marquez, R. & Meyer, A. Stereocontrolled total synthesis of (−)-callipeltoside A. *Org. Lett.* **5**, 4477–4480 (2003).
85 Narasaka, K. & Pai, F.-C. Stereoselective reduction of β hydroxyketones to 1,3-diols highly selective 1,3-asymmetric induction via boron chelates. *Tetrahedron* **40**, 2233–2238 (1984).
86 Wipf, P. & Graham, T. H. Synthesis of the C1′-C11′ segment of leucascandrolide A. *J. Org. Chem.* **66**, 3242–3245 (2001).
87 Burgess, E. M., Penton, H. R. & Taylor, E. A. Thermal reactions of alkyl *N*-carbomethoxysulfamate esters. *J. Org. Chem.* **38**, 26–31 (1973).
88 Irschik, H., Jansen, R., Gerth, K., Höfle, G. & Reichenbach, H. Chivosazole A, a new inhibitor of eukaryotic organisms isolated from myxobacteria. *J. Antibiot. (Tokyo)* **48**, 962–966 (1995).
89 Jansen, R., Irschik, H., Reichenbach, H. & Höfle, G. Chivosazoles A–F: novel antifungal and cytotoxic macrolides from *Sorangium cellulosum* (Myxobacteria). *Liebigs Ann* **1997**, 1725–1732 (1997).
90 Diestel, R. *et al.* Chivosazoles A and F, cytostatic macrolides from myxobacteria, interfere with actin. *ChemBioChem* **10**, 2900–2903 (2009).
91 Yeung, K.-S. & Paterson, I. Actin-binding marine macrolides: total synthesis and biological importance. *Angew. Chem. Int. Ed.* **41**, 4632–4653 (2002).
92 Janssen, D., Albert, D., Jansen, R., Müller, R. & Kalesse, M. Chivosazole A—elucidation of the absolute and relative configuration. *Angew. Chem. Int. Ed.* **46**, 4898–4901 (2007).
93 Brodmann, T., Janssen, D. & Kalesse, M. Total synthesis of chivosazole F. *J. Am. Chem. Soc.* **132**, 13610–13611 (2010).
94 Williams, S. *et al.* An expedient total synthesis of chivosazole F: an actin-binding antimitotic macrolide from the myxobacterium *Sorangium cellulosum*. *Angew. Chem. Int. Ed.* **56**, 645–649 (2017).
95 Paterson, I. *et al.* Enantio- and diastereoselective aldol reactions of achiral ethyl and methyl ketones with aldehydes: the use of enol diisopinocampheylborinates. *Tetrahedron* **46**, 4663–4684 (1990).
96 Paterson, I., Goodman, J. M. & Isaka, M. Aldol reactions in polypropionate synthesis: high π-face selectivity of enol borinates from α-chiral methyl and ethyl ketones under substrate control. *Tetrahedron Lett.* **30**, 7121–7124 (1989).
97 Phillips, A. J., Uto, Y., Wipf, P., Reno, M. J. & Williams, D. R. Synthesis of functionalized oxazolines and oxazoles with DAST and deoxo-Fluor. *Org. Lett.* **2**, 1165–1168 (2000).
98 Campbell, A. D., Paterson, D. E., Taylor, R. J. K. & Raynham, T. M. exo-Glycal approaches to C-linked glycosyl amino acid synthesis. *Chem. Commun.* 1599–1600 (1999).
99 Kitamura, M., Tokunaga, M., Ohkuma, T. & Noyori, R. Convenient preparation of BINAP-ruthenium(II) complexes catalyzing asymmetric hydrogenation of functionalized ketones. *Tetrahedron Lett.* **32**, 4163–4166 (1991).
100 Duplantier, A. J. & Masamune, S. Pimaricin. Stereochemistry and synthesis of its aglycon (pimarolide) methyl ester. *J. Am. Chem. Soc.* **112**, 7079–7081 (1990).
101 Paterson, I., Gibson, L. J. & Kan, S. B. J. Synthesis of the C15 – C35 northern hemisphere subunit of the chivosazoles. *Org. Lett.* **12**, 5530–5533 (2010).
102 Shirokawa, S. I. *et al.* Remote asymmetric induction with vinylketene silyl N,O-acetal. *J. Am. Chem. Soc.* **126**, 13604–13605 (2004).
103 Paterson, I., Kan, S. B. J. & Gibson, L. J. Synthesis of the C1 – C13 tetraenoate subunit of the chivosazoles. *Org. Lett.* **12**, 3724–3727 (2010).
104 Littke, A. F., Schwarz, L. & Fu, G. C. Pd/P(t-Bu)3: a mild and general catalyst for Stille reactions of aryl chlorides and aryl bromides. *J. Am. Chem. Soc.* **124**, 6343–6348 (2002).
105 Ando, K. Highly selective synthesis of Z-unsaturated esters by using new Horner–Emmons reagents, ethyl (diarylphosphono)acetates. *J. Org. Chem.* **62**, 1934–1939 (1997).
106 Still, W. C. & Gennari, C. Direct synthesis of Z-unsaturated esters. A useful modification of the Horner–Emmons olefination. *Tetrahedron Lett.* **24**, 4405–4408 (1983).
107 Paterson, I. & Lyothier, I. Total synthesis of (+)-discodermolide: an improved endgame exploiting a Still–Gennari-type olefination with a C1-C8 α-ketophosphonate fragment. *Org. Lett.* **6**, 4933–4936 (2004).